



Evolutionary genomics of gypsy moth populations sampled along a latitudinal gradient

Christopher J. Friedline¹ | Trevor M. Faske¹ | Brandon M. Lind²  | Erin M. Hobson¹ | Dylan Parry³ | Rodney J. Dyer⁴ | Derek M. Johnson¹ | Lily M. Thompson⁵ | Kristine L. Grayson⁵ | Andrew J. Eckert¹ 

¹Department of Biology, Virginia Commonwealth University, Richmond, Virginia

²Integrative Life Sciences Ph.D. Program, Virginia Commonwealth University, Richmond, Virginia

³Department of Environmental & Forest Biology, State University of New York, Syracuse, New York

⁴Center for Environmental Studies, Virginia Commonwealth University, Richmond, Virginia

⁵Department of Biology, University of Richmond, Richmond, Virginia

Correspondence

Andrew J. Eckert, Department of Biology, Virginia Commonwealth University, Richmond, VA.
Email: aeckert2@vcu.edu

Funding information

Thomas F. and Kate Miller Jeffress Memorial Trust

Abstract

The European gypsy moth (*Lymantria dispar* L.) was first introduced to Massachusetts in 1869 and within 150 years has spread throughout eastern North America. This large-scale invasion across a heterogeneous landscape allows examination of the genetic signatures of adaptation potentially associated with rapid geographical spread. We tested the hypothesis that spatially divergent natural selection has driven observed changes in three developmental traits that were measured in a common garden for 165 adult moths sampled from six populations across a latitudinal gradient covering the entirety of the range. We generated genotype data for 91,468 single nucleotide polymorphisms based on double digest restriction-site associated DNA sequencing and used these data to discover genome-wide associations for each trait, as well as to test for signatures of selection on the discovered architectures. Genetic structure across the introduced range of gypsy moth was low in magnitude ($F_{ST} = 0.069$), with signatures of bottlenecks and spatial expansion apparent in the rare portion of the allele frequency spectrum. Results from applications of Bayesian sparse linear mixed models were consistent with the presumed polygenic architectures of each trait. Further analyses indicated spatially divergent natural selection acting on larval development time and pupal mass, with the linkage disequilibrium component of this test acting as the main driver of observed patterns. The populations most important for these signals were two range-edge populations established less than 30 generations ago. We discuss the importance of rapid polygenic adaptation to the ability of non-native species to invade novel environments.

KEYWORDS

ddRADseq, double digest restriction-site associated DNA sequencing, evolutionary genomics, genome-wide associations, *Lymantria dispar*, polygenic adaptation

1 | INTRODUCTION

Biological invasions are useful natural experiments with which to test hypotheses about evolutionary responses to novel environments (Baker & Stebbins, 1965; Keller & Taylor, 2008; Suarez &

Tsutsui, 2008). This applies to the original colonization event, as well as the post-colonization range expansion characteristic of invasive species. Examples abound of phenotypic and genetic differentiation between native and introduced ranges, as well as across introduced ranges, for a variety of plant and animal taxa (reviewed

by Coulatti & Lau, 2015; Dlugosch & Parker, 2008; Dlugosch, Anderson, Braasch, Cang, & Gillette, 2015). These examples define a paradox, known as the “genetic paradox of invasion,” whereby the establishment and subsequent expansion into novel environments presumably dominated by populations of locally adapted native species should be extremely unlikely, yet there are abundant examples of widespread and successful invasions of exotic species across all forms of life (Allendorf & Lundquist, 2003). At its core, this paradox, if indeed it even exists (Estoup et al., 2016), is defined by a set of evolutionary questions related to the efficiency of natural selection, created through novel environmental drivers acting upon genetic variation within nonequilibrium populations, to effect evolutionary change (see figure 3 in Estoup et al., 2016; cf. Baker & Stebbins, 1965). Here, we use the invasion of the European gypsy moth (*Lymantria dispar* L.) across eastern North America to test hypotheses about the genetic architecture of local adaptation at range margins.

Range margins, even for invasive species, can present novel and extreme environments relative to those in the range centre or area of initial colonization (Keller & Taylor, 2008). A standing body of literature has examined the consequences of evolution within peripheral populations of species near their range limits (reviewed by Eckert, Samis, & Lougheed, 2008). Peripheral populations often display reduced variation within populations (e.g., Blows & Hoffmann, 1993), greater differentiation among populations (e.g., Kunin et al., 2009) and increased levels of segregating deleterious variation (e.g., Lohmueller et al., 2008). Although these trends have been noted repeatedly and have led to the conclusion that adaptive evolution within peripheral populations can be limited (but see, for exceptions, Hill, Griffiths, & Thomas, 2011; Therry, Nilsson-Örtman, Bonte, & Stoks, 2014), additional work has identified differences between leading and lagging peripheral populations as repositories for fitness-related standing genetic variation (Rehm, Olivas, Stroud, & Feeley, 2015; e.g., Keller, Chhatre, & Fitzpatrick, 2017). Peripheral populations can also display greater independence among phenotypic traits in multivariate space, leading to reductions in constraints imposed by fitness trade-offs (Caley, Cripps, & Game, 2013; Paccard, Buskirk, & Willi, 2016), as well as maintain quantitative genetic variation for fitness-related phenotypic traits even when neutral genetic markers display reductions in diversity (Dlugosch et al., 2015). While it is unclear if these trends universally apply to invasive species (Guo, 2014), as many of these patterns use assumptions about stabilities and relationships between abundances and the structure of geographical ranges (Sagarin, Gaines, & Gaylord, 2006), it is reasonable to expect that post-colonization expansion by invasive species will result in exposure to environments that provide novel and often strong selection pressures (reviewed by Coulatti & Lau, 2015).

Examples of rapid adaptation to novel environments are frequent within the literature (e.g., Cook & Saccheri, 2013; Crossley, Chen, Groves, & Schoville, 2017; Grant & Grant, 2008). These examples exhibit a range in underlying genetic architectures, from those characterized by a few major-effect loci (e.g., van't Hof, Edmonds,

Dalikova, Marec, & Saccheri, 2011) to those of many underlying loci (e.g., Lamichhane et al., 2015). Theoretical studies and reviews have highlighted that rapid adaptation to novel environments can proceed rapidly via soft sweeps acting on polygenic architectures composed of alleles already present within populations (e.g., Berg & Coop, 2014; Pritchard & Di Rienzo, 2010; Le Corre & Kremer, 2012). This occurs for several reasons. For example, there is no lag between environmental change and the origin of adaptive variation, because the alleles are already segregating within populations. Novel mutations that have large effects on phenotypes are also likely to be disadvantageous and swept from the population (Orr, 2005), while alleles comprising standing genetic variation are probably found within multiple individuals and/or populations and have been previously sorted based on their fitnesses across various genetic backgrounds (reviewed by Barrett & Schluter, 2008; Hermisson & Pennings, 2005; Hermisson & Pennings, 2017). Thus, rapid adaptation via soft sweeps is probably very common for traits underlain by polygenic architectures. Moreover, these sweeps are often driven not by strong allele frequency differences, but instead by subtle, coordinated allele frequency changes across populations (Chevin & Hospital, 2008; Jain & Stephan, 2015, 2017).

Ectothermic organisms, like the gypsy moth, experience fluctuations in development rate, mass, fecundity and survival as a direct response to temperature. Typically, these responses have negative fitness consequences when exposed to temperatures over their optimum (Kingsolver & Woods, 1997; Limbau et al., 2017; Logan, Casagrande, & Liebhold, 1991; Thompson et al., 2017). For example, range retraction along the southern invasion front of the gypsy moth coincides with geographical areas having a higher frequency of supraoptimal temperatures (Tobin, Gray, & Liebhold, 2014), which implies that these temperatures impart fitness costs. Controlled laboratory experiments, moreover, have shown that gypsy moths reared at higher temperatures experience reduced pupal mass and increased development times (Logan et al., 1991; Thompson et al., 2017), both of which are likely to lower fitness (Calvo & Molina, 2005; Honěk, 1993; Myers, Malakar, & Cory, 2000). Low temperatures have also been shown to have negative consequences for development in European gypsy moth, with some populations displaying patterns of adaptive variation (Fält-Nardmann, Klemola, et al., 2018; Fält-Nardmann, Ruohomäki, Tikkanen, & Neuvonen, 2018). In general, these traits are also heritable, with those related to development time and pupal mass having heritabilities varying from 0.181 to 0.703 (Janković-Tomanić & Lazarević, 2012; Lazarević, Nenadović, Janković-Tomanić, & Milanović, 2008; Lazarević, Perić-Mataruga, Ivanović, & Anđelković, 1998; Lazarević, Perić-Mataruga, Stojković, & Tucić, 2002; Lazarević, Perić-Mataruga, & Tucić, 2007; Páez, Fleming-Davies, & Dwyer, 2015). Thus, phenotypic traits related to pupal mass and development time could be the targets of natural selection, particularly at the invasion fronts where thermal regimes limit larval and pupal development.

The combination of its broad geographical range, known locality and year of introduction and extremely well-documented

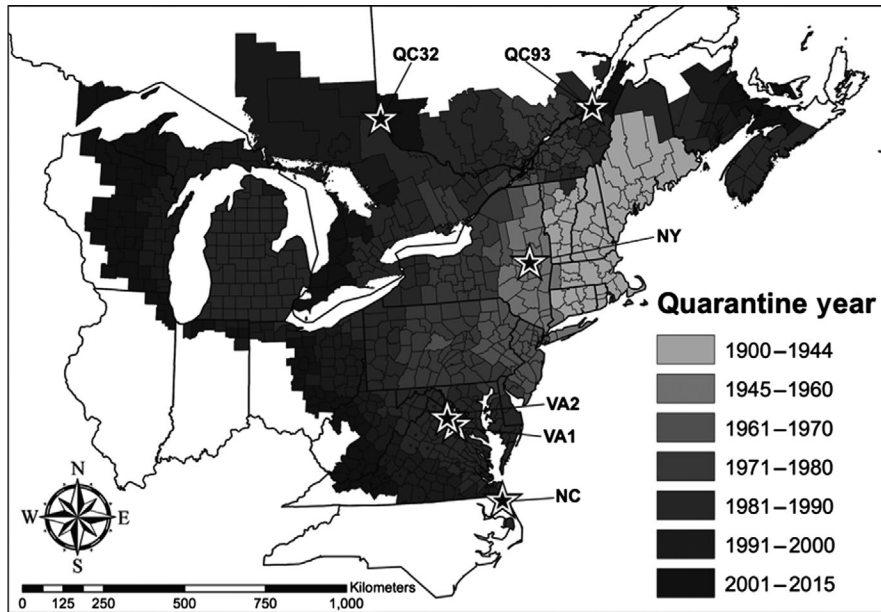


FIGURE 1 Sampling locations relative to the timing of county-wide quarantine year across the introduced range of European gypsy moth (*Lymantria dispar*) in eastern North America. Sample sizes for each sampled population are given in Table 1

spatial spread (Bogdanowicz, Mastro, Prasher, & Harrison, 1997; Grayson & Johnson, 2017; Liebhold, Halverson, & Elmes, 1992; Liebhold, Mastro, & Schaefer, 1989; Tobin, Bai, Eggen, & Leonard, 2012; Wu et al., 2015) make the gypsy moth an ideal model for examining the genetic architecture of local adaptation in response to recent range expansion and novel environmental pressures. Here, we focus on a set of populations sampled across the invaded latitudinal range of North America. Using a combination of genomics, common garden experimentation (i.e., the raising and study of individuals in a standard environment) and evolutionary genetic inferences, we test the hypothesis that range edge populations of gypsy moth are experiencing divergent selective pressures on polygenic traits related to thermal tolerance during larval and pupal development. Our results indicate that locally adapted populations at the range margins evolved rapidly (<30 generations) through subtle and coordinated allele frequency shifts at trait-associated loci. We extend our results to a

discussion of rapid evolution and its consequences for biological invasions.

2 | MATERIALS AND METHODS

2.1 | Field collections and laboratory rearing

We established populations of gypsy moth from across the latitudinal range of the invasion in North America (Figure 1) in autumn 2011 by collecting egg masses from Quebec (QC32 and QC93), New York (NY), Virginia (VA1 and VA2) and North Carolina (NC). Collections were made between 2011 and 2012. Within populations, sampling of more than one egg mass in close spatial proximity (e.g., the same tree) was avoided, to minimize collections enriched for close relatives. All collected egg masses ($n = 25\text{--}33$ per population) were surface sterilized with 10% formalin before rearing to remove pathogens. To protect against confounding maternal effects from population density or

TABLE 1 Summary of sampled populations

	Population					
	NC	VA1	VA2	NY	QC93	QC32
Latitude	36.44913	38.65761	38.85747	42.89777	46.90826	47.25098
Longitude	-76.02467	-77.46360	-77.69500	-74.09476	-70.80611	-79.40605
Sample size	21	32	32	22	25	33
$\overline{\text{Mass}}(SD)$	0.299 (0.044)	0.296 (0.086)	0.274 (0.037)	0.296 (0.049)	0.252 (0.056)	0.300 (0.043)
$\overline{\text{PDT}}(SD)$	10.762 (1.513)	10.438 (1.294)	10.188 (1.330)	11.136 (1.521)	9.960 (1.457)	10.788 (1.556)
$\overline{\text{LDT}}(SD)$	66.571 (4.872)	63.531 (4.928)	61.781 (4.526)	61.955 (3.337)	60.320 (4.037)	62.242 (3.046)
$\overline{H_{\text{OBS}}}(SD)$	0.244 (0.192)	0.246 (0.167)	0.239 (0.181)	0.241 (0.190)	0.245 (0.191)	0.253 (0.180)
$\overline{H_{\text{EXP}}}(SD)$	0.248 (0.176)	0.261 (0.165)	0.249 (0.174)	0.246 (0.175)	0.249 (0.177)	0.258 (0.170)

Note. H_{EXP} , expected heterozygosity; H_{OBS} , observed heterozygosity; SD, standard deviation.

host quality (Rossiter, 1991), we reared each population through one generation on northern red oak (*Quercus rubra* L.) foliage in an outdoor array under ambient temperatures at Lafayette Road Field Station in Syracuse, NY (43.0481°N, 76.1474°W) during spring 2012. Egg masses from 20–40 females were broken apart and mixed together to homogenize genetic diversity and 100–150 neonates were drawn from this pool at hatching. First and second instars were initially housed in large plastic Petri dishes and transferred as 3rd instars to 18.9-L plastic buckets covered with a spun polyester mesh. Larvae were exclusively fed fresh cut *Q. rubra* foliage every 3–4 days until pupation, with all larvae from all populations receiving foliage from the same tree on the same day. Emerged adults were placed in paper-lined buckets for mating and oviposition of eggs for the next generation. Resulting eggs were overwintered under outdoor conditions at the rearing location.

2.2 | Phenotypic measurements

In spring 2013, the F_2 generation eggs for all six populations were transported to Virginia Commonwealth University, Richmond, VA, for a common garden experiment conducted at the VCU Rice Rivers Center (37.3265°N, 77.2056°W). Overwintering eggs were allowed to hatch in synchrony with budburst of *Q. rubra* at each site. Hatched larvae were selected at random to minimize relatedness and placed into a large plastic Petri dish with fresh foliage, changed every 3–4 days gathered from the same tree on the same day. After reaching 3rd instar, larvae were reallocated to four replicate 18.9-L plastic buckets and covered with a spun polyester mesh fabric for each population at densities of $n = 30$ larvae per bucket. Each cup/bucket contained *Q. rubra* stems with leaves placed in a 3.9-L plastic jug filled with water. Larvae were checked for pupation daily, and fully sclerotized pupae were weighed and stored in paper lined 74-ml plastic cups with snap cap lids punched with pinholes for air exchange. Pupae were checked daily for adult emergence with sex and date being recorded. Only males were included in analyses because they are the sex captured in pheromone-baited traps placed in an extensive network across the invasion front to monitor spread annually (Sharov, Leonard, Liebhold, Roberts, & Dickerson, 2002). The phenotypes measured were pupal mass (Mass) in grams, larval development time (LDT: hatching to pupation) in days and pupal duration (PD: pupation to adult emergence) in days, as these are commonly measured components of early life survival for gypsy moth (see Introduction1 and Discussion).

2.3 | Library preparation, sequencing and data processing

We used a two-step approach to discover and characterize variants across the gypsy moth genome: (a) creation of a reference assembly from a single caterpillar and (b) reduced representation genotype-by-sequencing of 192 moths sampled from six natural populations (Table 1; Figure 1). Total genomic DNA was extracted from all 192 moths using Qiagen DNeasy Blood and Tissue kits (Qiagen) following the manufacturer's protocol. A reference assembly was constructed from a reference caterpillar (source population = NY), while the other

192 moths were subjected to a double digest restriction site-associated DNA sequencing (ddRADseq) protocol (Parchman et al., 2012; see also Picq et al., 2018 for a similar approach). A single run of paired-end reads on the Illumina HiSeq 2,500 platform at the Virginia Commonwealth University Nucleic Acids Research Facility was used to generate data for the reference assembly. The read pairs were each evaluated along sliding windows of 5 bp. If the mean quality score in this window was below 30, the read was trimmed at that beginning of the window. If the shortened read was less than 50% of the length of the original read, it was discarded along with its pair. Additionally, if 20% of the bases in a read had quality values less than 30, it was discarded along with its pair. For ddRADseq libraries, 96 samples were multiplexed and each library ($n = 2$ libraries) was sequenced using a single lane on the Illumina HiSeq 2500 platform at the same facility. Quality of all reads was initially assessed using FASTQC (Babraham Bioinformatics 2015) and subsequently processed with IPYTHON (Pérez & Granger, 2007) and BIOPYTHON (Cock et al., 2009). The same protocol was used to filter single-end reads resulting from sequencing of the multiplexed, ddRADseq libraries as the reference assembly.

2.4 | Creation and annotation of a reference assembly

The quality-filtered reads from the paired-end sequencing library, which represented a single moth, were used as input to the MASURCA assembler (Zimin et al., 2017), with the following parameters changed from the defaults: mean/standard deviation of read length: 400/60, use linking mates: 1: cgwErrorRate: 0.15. The quality of the assembly was assessed using the statistics generated by the assembly process, as well as with BUSCO (Simão, Waterhouse, Ioannidis, Kriventseva, & Zdobnov, 2015) and QUASt (Gurevich, Saveliev, Vyahhi, & Tesler, 2013). For BUSCO, the assembly was evaluated against pre-computed Augustus (Stanke & Waack, 2003) meta-parameters of three species (*Aedes*, *Heliconius* and *Drosophila*) and the BUSCO Arthropoda lineage profile using a *tblastn* e-value cut-off of 0.001. For QUASt, the software was executed using the following options (--gene-finding, --eukaryote, --glimmer, --min-contig 200).

The MAKER genome annotation pipeline (Cantarel et al., 2008) version 2.31.8 was used to predict the gene content of the assembly (Campbell, Holt, Moore, & Yandell, 2014). Auxiliary programs that were used as part of the MAKER suite were NCBI BLAST+ version 2.2.28 (Camacho et al., 2009), REPEATMASKER version open-4.0.5 (Smit, Hubley, & Green, 2015), EXONERATE version 2.2.0 (Slater & Birney, 2005), SNAP version 2006-07-28 (Korf, 2004), GENEMARK-ES version 3.49 (Ter-Hovhannisyan, Lomsadze, Chernoff, & Borodovsky, 2008), AUGUSTUS version 3.2.2 (Stanke, Steinkamp, Waack, & Morgenstern, 2004), TRNASCAN-SE version 1.3.1 (Lowe & Eddy, 1997) and PROBUILD version 2.36. The *Heliconius melpomene* version 2 genome was provided as both expressed sequence tag (EST) and protein homology evidence in addition to the AUGUSTUS supplied *heliconius_melpomene1* set of species parameters. Resulting annotations were used to define categories (i.e., annotation categories) for contigs containing single nucleotide

polymorphisms (SNPs) corresponding to genic, varying distances to genes (500, 1,000 and 1,500 bp), intergenic, repetitive and unknown (Supporting Information Appendix S1).

2.5 | Variant calling and genotype determination

FASTQ files resulting from single-end sequencing of the ddRADseq libraries were demultiplexed using GBSX (Herten, Hestand, Vermeesch, & Houdt, 2015) version 1.2, allowing two mismatches (-mb 2). We allowed two mismatches during this process, because our barcodes were designed to have four mismatches (Parchman et al., 2012), as a sensible compromise between stringency and the need to achieve enough coverage to call genotypes for each sample. Demultiplexed reads were subsequently mapped to a reference assembly of 277,541 contigs using BOWTIE2 version 2.2.4 (Langmead & Salzberg, 2012), with flags --local --very-sensitive-local. The flag --N, however, was set to 1 from the default of 0. These options were used to increase the sensitivity of the alignment steps (see the BOWTIE manual for more information). The resulting SAM files were converted to their binary equivalent (BAM), sorted and indexed using SAMTOOLS version 1.2 (Li et al., 2009). PICARD version 1.112 (<https://broadinstitute.github.io/picard>) was used to annotate each BAM with read group and sample informational tags. Sequence variants were called from the resulting BAM files using SAMTOOLS and BCFTOOLS version 1.3.1 (Li et al., 2009). The variants were filtered using VCFTOOLS (Danecek et al., 2011), such that only SNPs that were biallelic (--min-alleles = 2, --max-alleles = 2) and present in at least 50% of the samples (--max-missing = 0.5) were kept. Additional filtering using custom PYTHON scripts removed samples lacking sufficient genetic and phenotypic data ($n = 27$ moths removed). The filtering protocol kept SNPs with minor allele frequency (MAF) of at least 1%, depth across samples (DP) ≥ 100 or DP < 1,500, alternate allele call quality (QUAL) ≥ 20 , and the absolute value of Wright's $F < 0.50$. These filters were selected to minimize the occurrence of variants derived from paralogous loci (e.g., DP < 1,500, Wright's F), remove variants arising from errors during mapping or sequencing (e.g., QUAL, MAF), and remove those for which the imputation steps for some statistical analyses (e.g., principal components analysis [PCA]) would require imputing more than half the data (e.g., DP ≥ 100 , missing data threshold of 0.50).

To account for uncertainty in genotype determination for the genome-wide association analyses, weighted genotypes (G_W) were calculated by converting the Phred-scaled likelihoods in the VCF file to weights (W_i) for the 0, 1 and 2 genotype calls (G_i):

$$G_W = \sum_{i=1}^3 G_i \times W_i$$

where the W_i were scaled by the sum of the three likelihoods. Considering our liberal threshold for the percentage of samples with missing data (50%), a custom imputation protocol was also implemented. Allele frequencies within each population were estimated for each SNP from the weighted genotypes, Hardy-Weinberg equilibrium (HWE) was assumed and the HWE proportions were assigned as the weights in the equation above to determine a weighted

genotype call for a specific sample at a specific SNP. This procedure was applied only to those samples for which the Phred-scaled likelihoods for an SNP were zero or undefined because of a complete lack of data. Imputed data of this form were used solely for the genome-wide association analyses.

2.6 | Patterns of phenotypic and genetic variation

Differentiation among populations for phenotypic traits was assessed using multivariate analysis of variance (MANOVA). Statistical significance of the MANOVA model was determined using Wilk's λ as the test statistic and $\alpha = 0.05$ as a significance threshold. We subsequently used one-way analysis of variance (ANOVA) to assess differentiation separately for each phenotypic trait. Post hoc tests for the differences in population means for each phenotypic trait were performed using Tukey's honest significant difference (HSD) method assuming $\alpha = 0.05$. We treated populations as a fixed effect for statistical hypothesis testing ($\alpha = 0.05$), but as a random effect for estimation of variance components. Variance components were used to construct a measure of phenotypic differentiation akin to hierarchical F -statistics. Specifically, we used the ratio of the variance accounted for by populations to the total phenotypic variance (P_{ST}) as a measure of phenotypic differentiation. Parametric bootstrapping ($n = 1,000$ replicates) was used to derive confidence intervals around point estimates of P_{ST} . All analysis was conducted using the STATS version 3.4.0 and LME4 version 1.1-13 libraries in R version 3.4.0 (Bates, Mächler, Bolker, & Walker, 2015; R Core Team, 2017).

Patterns of genetic variation within and among populations were described using standard population genetic indices: heterozygosities (observed and expected heterozygosities, H_{OBS} and H_{EXP} respectively) and hierarchical F -statistics. We also quantified the number and frequency of private alleles within populations (i.e., alleles unique to a single population) to identify recent demographic events (Luikart, Allendorf, Cornuet, & Sherwin, 1998). Estimates of hierarchical F -statistics were made for each SNP and all SNPs combined using the HIERFSTAT version 0.04-22 library in R. Confidence intervals (95%) for multilocus estimates were generated using bootstrapping across SNPs ($n = 1,000$ replicates). For comparison, genetic structure was also assessed using PCA following Patterson, Price, and Reich (2006).

We used redundancy analysis (RDA) and Mantel tests to investigate the effects of genetics and geography on phenotypic trait values. We partitioned the explainable variance in phenotypic trait values by genetics and geography using standard partitioning methods (Borcard, Legendre, & Drapeau, 1992), which required definition of full (i.e., phenotypic trait values ~ genetics + geography) and partial RDA (pRDA) models (e.g., phenotypic trait values ~ genetics | geography). Geography was quantified using latitude and longitude, with both measures centred and standardized prior to analysis, while genetic effects were quantified using PCs derived from PCA. The statistical significance of all RDA models ($\alpha = 0.05$), as well as RDA axes within these models, was tested using a permutation-based ANOVA with 999 permutations (Legendre & Legendre, 2012). For comparison,

Mantel tests were conducted using pairwise F_{ST} as the genetic distances, great circle distances (km) as the geographical distances and Euclidean distances, calculated from centred and standardized phenotypic trait values, as the phenotypic trait distances. Statistical significance of the observed correlation values was assessed using 999 permutations (see Legendre, Fortin, & Borcard, 2015 for concerns with hypothesis tests of Mantel's r as they relate to hypothesis tests of the original data). All analyses were performed using functions in the VEGAN version 2.4–3 library of R (Oksanen et al., 2017).

2.7 | Genome-wide association analyses

We used Bayesian sparse linear mixed models (BSLMMs) to associate phenotypes with genotypes at 85,162 of the 91,468 SNPs (Zhou, Carbonetto, & Stephens, 2013). We dropped 6,306 SNPs from this analysis because the amount of missing data for these SNPs, even with the imputation scheme described above, was above a threshold of 5%. This was due to cases where all samples, comprising at least 5% of the total sample size, were missing in at least one population for an SNP, so that population-level allele frequencies were not available for imputation. In this framework, multi-SNP models, where the set of predictive SNPs is itself a parameter, are fit to each phenotype using a Bayesian implementation of a sparse linear mixed model. In this model, effects of SNPs are partitioned into polygenic effects (α) and sparse effects (β). The total effect of each SNP is then the sum of its polygenic effect and its sparse effect weighted by the posterior inclusion probability (PIP) of it in the multi-SNP model (γ). Confounding due to relatedness among individuals was addressed through use of a relatedness matrix (K), which is an $n \times n$ matrix of standardized relatedness estimates that is estimated from the genotype data.

Parameters of the BSLMMs were estimated using a Markov chain Monte Carlo (MCMC) procedure. The parameters of interest were the effect sizes for each SNP, as well as three hyperparameters: the proportion of phenotypic variance explained by sparse and polygenic effects (PVE), the proportion of genetic variance explained by sparse effects (PGE) and the number of SNPs retained in the predictive model relating genotypes to phenotypes (N). A separate BSLMM was fit to the normal-quantile-transformed data for each phenotype using five MCMC chains. After a burn-in of 1,000,000 steps, each MCMC chain was run for an additional 20,000,000 steps with parameter estimates sampled every 1,000 steps. Associated SNPs for each phenotypic trait were defined as those in the upper (99.95%) and lower (0.05%) tails of the total effect size distribution across all 85,162 analysed SNPs. Each phenotypic trait thus had a set of 86 associated SNPs, 43 of which had negative effects of the minor allele on the phenotypic trait value and 43 of which had positive effects. Fitting and analysis of BSLMMs were conducted using the GEMMA software (Zhou & Stephens, 2012), with assessment of convergence for the MCMC carried out using the CODA library in R (Plummer, Best, Cowles, & Vines, 2006). Parameter and hyperparameter estimates are given as the average across five independent MCMC runs.

2.8 | Evolutionary genetics of associated loci

Given that the sampled populations are distributed across broad environmental gradients known to affect the phenotypic traits we measured (Logan et al., 1991; Thompson et al., 2017; Tobin et al., 2014), we tested for signatures of divergent natural selection across populations using the approach developed by Berg and Coop (2014). R scripts for this analysis were obtained from <https://github.com/jjberg2/PolygenicAdaptationCode>. Using the total effect sizes estimated for each associated SNP, their frequencies within each population and a variance–covariance matrix of allele frequencies across populations describing neutral processes (e.g., genetic drift), Berg and Coop (2014) defined an excess variance test using a statistic closely related to Q_{ST} . This statistic, Q_X , is defined by two terms. One term quantifies allele frequency differences among populations (i.e., an F_{ST} component), while the other term quantifies linkage disequilibrium (LD) among loci across populations (i.e., an LD component). The latter encapsulates subtle and coordinated allele frequency shifts across populations. The null distribution of Q_X is created through sampling of SNPs unassociated with each of the phenotypic traits. These SNPs are matched to those associated with the phenotypic traits based on minor allele frequency (25 bins ranging from 0 to 0.50) and are used to estimate the variance–covariance matrix describing neutral processes and the null distribution of genetic values used to estimate a null distribution of Q_X . We followed Berg and Coop (2014) and used 20,000 SNPs for estimation of the variance–covariance matrix and 10,000 SNPs to create the null distribution of Q_X . The variance–covariance matrix was estimated 10 times (i.e., 10 matrices each estimated using 20,000 random SNPs), with the average being used as the final representation of neutral genetic structure for this methodology. Ten sets of null genetic values ($n = 10,000$ values per set) were also estimated for each phenotypic trait, so that the final null distributions of the test statistics were built from 100,000 values. We performed one-tailed tests for the observed value of Q_X being larger than expected by chance, including each of its components, based on these null distributions using a significance threshold of 0.05. Prior to analysis, we randomly selected one SNP per contig in the assembly to minimize confounding of LD signals due to physical linkage for a total of 38,658 SNPs.

We used Z-statistics from the method of Berg and Coop (2014) to examine which populations were contributing most to signals of divergent natural selection across populations. This test is defined by a null model in which the mean and variance of genetic values for a phenotypic trait within a focal population are predicted from the values observed in a reference set of populations and the variance–covariance matrix describing relationships among them. A Z-statistic is then estimated from the fit of the predicted values to the observed values in the focal population. Thus, rejection of this null model amounts to the focal population being an outlier relative to predictions based on the reference set of populations. Although this statistic is a standard normal deviate, we tested its significance using a two-tailed test based on the permutation approach as described for Q_X assuming a significance threshold of 0.05. For our analysis,

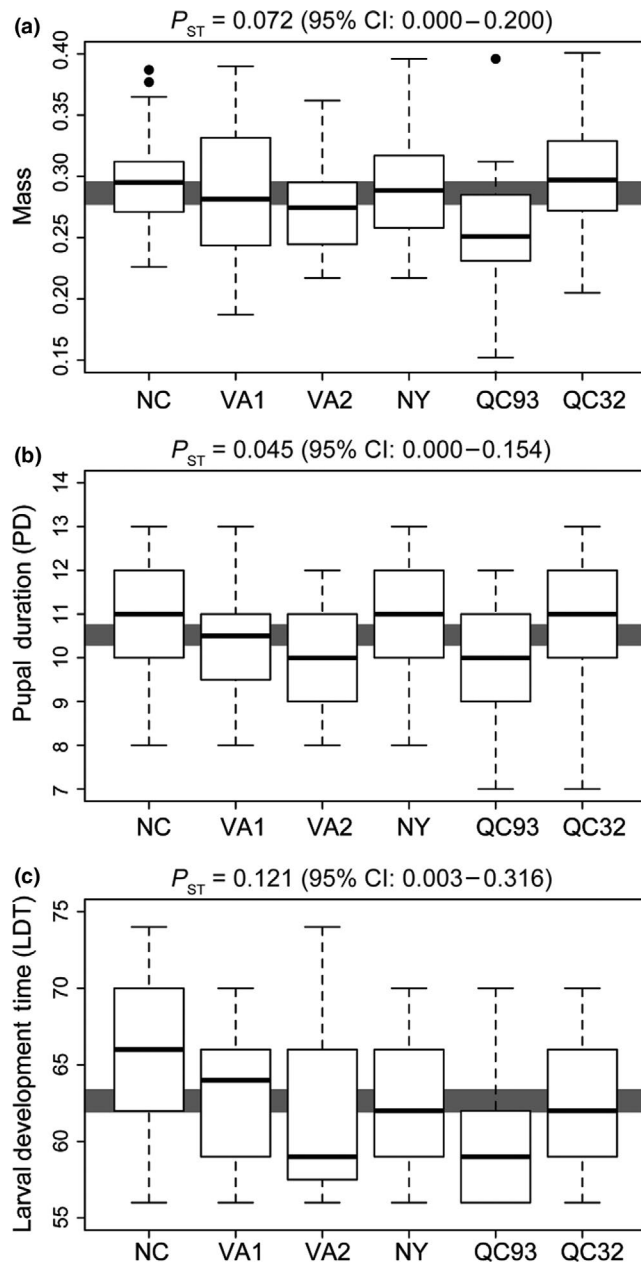


FIGURE 2 Phenotypic trait variation across populations is consistent with stronger differentiation for larval development time (LDT) relative to mass or pupal duration (PD). Whiskers for boxplots extend to 1.5 times the interquartile range. The horizontal grey band in each plot represents the 95% confidence interval for the global phenotypic trait mean (i.e., for all 165 samples). (a) Differentiation for mass across populations, which are ordered from south (left) to north (right), is weak to moderate, with marginal evidence of a latitudinal cline (Pearson's $r = -0.356$). A single outlier in the VA1 population with a mass of 0.671 g has been omitted from this graph, although all analysis includes this sample. (b) Differentiation for PD across populations, which are ordered from south (left) to north (right), is weak and not structured across latitude (Pearson's $r = -0.079$). (c) Differentiation for LDT across populations, which are ordered from south (left) to north (right), is moderate and structured across latitude (Pearson's $r = -0.600$). None of the correlations of phenotypic trait means to either geographical variable, however, was statistically significant

each population was dropped in turn (i.e., became the focal population), with the remaining five populations acting as the reference set.

3 | RESULTS

3.1 | Patterns of phenotypic and genetic variation

Phenotypic trait values varied across populations (Figure 2), with multivariate phenotypic trait values differing across populations (MANOVA: Wilk's $\lambda = 0.663$, $F_{15,433.81} = 4.647$, $p = 2.695 \times 10^{-8}$). Phenotypic trait values were moderately correlated across individuals (Pearson's $r = -0.524$ to 0.299). Inspection of results from one-way ANOVAs revealed that multivariate differentiation was driven largely by LDT ($F_{5,159} = 4.324$, $p = 0.001$), while Mass ($F_{5,159} = 3.062$, $p = 0.011$) and PD ($F_{5,159} = 2.272$, $p = 0.049$) were only marginally differentiated among populations. This was consistent with post hoc Tukey HSD tests, where there were four significant pairwise population differences for LDT (all involving NC except for the NC–VA1 comparison). In contrast, none to only a few of the population comparisons for PD ($n = 0$) and Mass ($n = 2$, QC93–QC32 and VA1–QC93) were significant. When taken together, these results were also consistent with point estimates of P_{ST} , where populations accounted for 12.13% (95% confidence interval [CI]: 0.30%–31.06%) of the variance for LDT, 7.17% (95% CI: 0.00%–20.00%) of the variance for Mass and 4.52% (95% CI: 0.00%–15.40%) of the variance for PD.

Genetic diversity within populations was geographically based (Figure 3) and indicative of a historical demography involving expansion from the point of initial introduction in Massachusetts. Mean observed heterozygosity (across SNPs) was positively correlated with latitude (Pearson's $r = 0.569$) and negatively correlated with longitude (Pearson's $r = -0.307$). Mean expected heterozygosity was negatively correlated with longitude (Pearson's $r = -0.605$) and weakly correlated with latitude (Pearson's $r = 0.061$). Heterozygosities also varied across annotation categories, with higher mean values outside of gene regions and in repeat regions (Supporting Information Figure S1). Variance within populations across loci for these measures also displayed geographical trends, although none of the correlations was statistically significant. All populations had private alleles ($n = 1,921$ SNPs with private alleles). The NY population had the fewest SNPs with private alleles ($n = 200$), whereas the QC32 population had the most ($n = 684$). In general, the number of SNPs with private alleles increased with geographical distance away from the NY population (Supporting Information Figure S2). The opposite pattern was apparent for the frequencies of private alleles, which were highest in the NY population (mean private allele frequency: 0.137, range = 0.025–0.444). The exception to this trend was the NC population (mean private allele frequency: 0.137, range = 0.025–0.344), with all other populations other than NY having lower mean frequencies of private alleles.

Genetic diversity was structured across populations, with the multilocus estimate of F_{ST} being 0.0690 (95% CI: 0.0686–0.0695). Single locus values of F_{ST} ranged from 0 to 0.483, with the majority

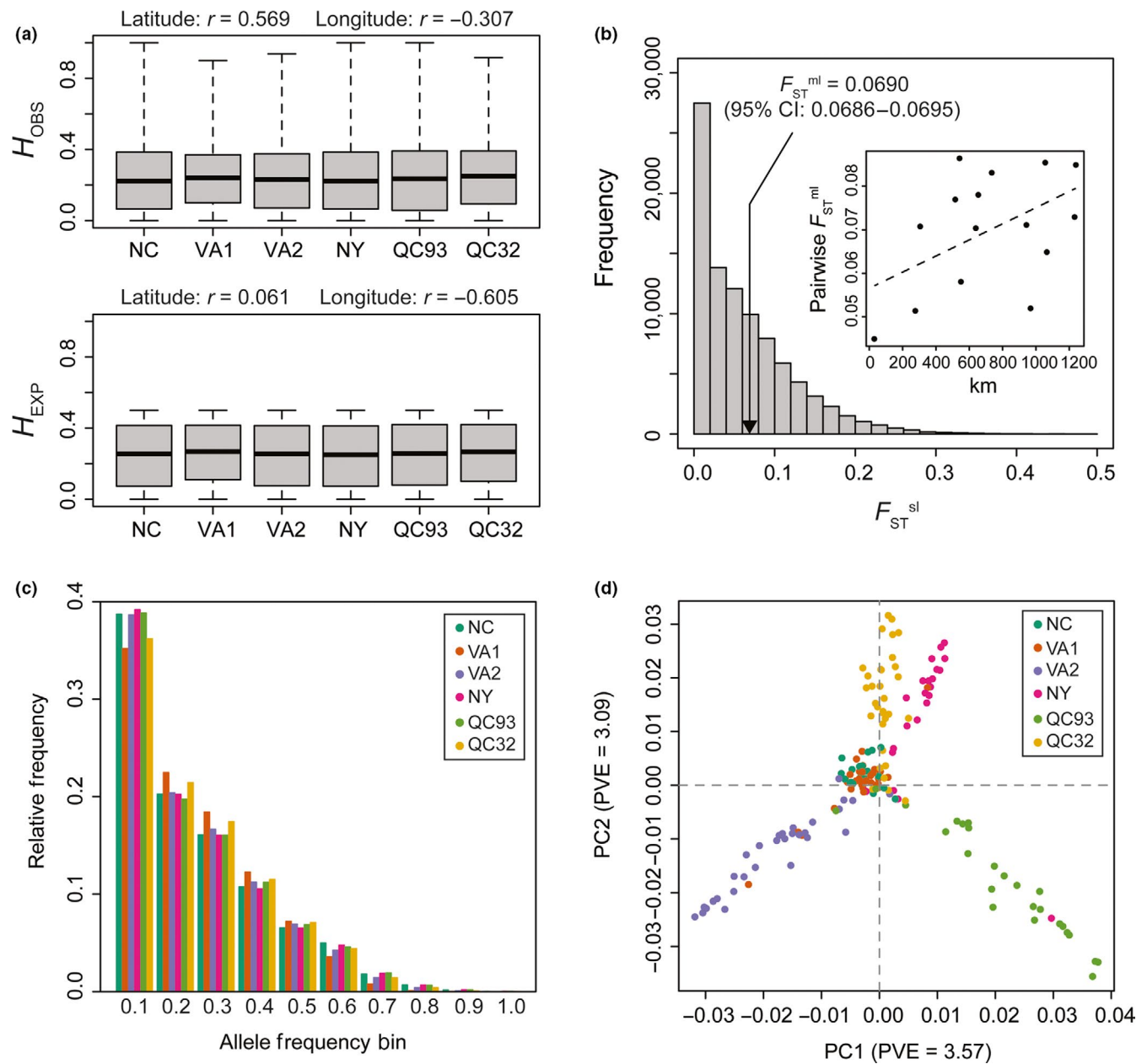


FIGURE 3 Patterns of genetic variation are structured among populations and are often clinal. (a) Central tendencies for the distributions of observed (H_{OBS}) and expected (H_{EXP}) heterozygosities do not differ greatly in magnitude among populations, although they are statistically different (Kruskal–Wallis tests: $p < 0.001$). Moderate correlations (Pearson's r) with latitude and longitude are also apparent for the means (given above each plot) and medians (not shown) of these distributions, although none of these correlations is statistically significant. (b) Populations of gypsy moths are differentiated genetically based on 91,468 SNPs, with the multilocus F_{ST} value (F_{ST}^{ml}) statistically greater than zero, and patterns of differentiation are consistent with isolation-by-distance (inset, Pearson's $r = 0.459$). Values of F_{ST} for single SNPs (F_{ST}^{sl}) ranged from 0 to 0.483. (c) Allele frequency spectra, based on 0.10 bins for the global minor allele within each population, are not strongly differentiated, as expected given the moderate value of F_{ST}^{ml} . The maximum of each bin is given as its label on the x-axis. (d) Principal components analysis (PCA) is consistent with differentiation among populations that is structured along latitudinal and longitudinal gradients. The top two principal components (PCs) jointly explain $\sim 6.66\%$ of the genetic variance (PVE). Scores for individual moths on each PC were scaled by the eigenvalue of that PC for plotting

(63.54%) of SNPs having single locus estimates of F_{ST} equal to or less than the multilocus value. Pairwise estimates of F_{ST} were structured geographically, with a statistically significant and positive relationship between F_{ST} and geographical distance (Mantel test: Pearson's $r = 0.459$, $p = 0.039$). Multilocus values for F_{ST} also

varied by annotation category, with lower values within gene regions (Supporting Information Figure S1). These patterns were also apparent in the PCA, where populations were clustered in the space defined by the first two principal components (PCs). These PCs explained 6.66% of the variance across samples and were correlated

with latitude and longitude (Pearson's r [latitude, longitude] = PC1: 0.650, 0.572; PC2: -0.414, 0.159; $p < 0.05$ for all correlations). Tracy–Widom tests of eigenvalues revealed that the top 17 PCs had p -values < 0.05 . Collectively, these 17 PCs explained 28.72% of the variance across individuals.

Phenotypic trait values were significantly correlated with geography and genetic variation (RDA: $F_{19,145} = 2.088$, $p = 0.001$, $R^2 = 0.215$, $R^2_{\text{adj}} = 0.112$; Table 2; Figure 4). All three RDA axes were statistically significant ($p < 0.010$). The first two RDA axes explained 87.18% of the total explainable variance (i.e., 87.18% of $R^2 = 0.215$). Partitioning the contribution of each type of variable to the overall explanatory power of the full RDA model revealed that genetic variation, as opposed to geography, had the largest pure effects on phenotypic trait variation (pure geography: 25.16%, pure genetics: 74.84%, confounded effects: 0.00%). This was consistent with the correlations among phenotypic, genetic and geographical distances, where geographical distances were significantly correlated with genetic distances (Figure 3b), phenotypic distances were significantly correlated with genetic distances (Mantel test: Pearson's $r = 0.511$, $p = 0.031$), but phenotypic distances were moderately, and not significantly, correlated with geography (Mantel test: Pearson's $r = 0.171$, $p = 0.273$). The pRDA models relating phenotypic variation to genetic variation conditional on geography and geography conditional on genetic variation were each statistically significant. The explanatory power between these two models, however, differed 3.10-fold (Table 2).

3.2 | Genome-wide association analyses

The structure of the relationship matrix (\mathbf{K}), as assessed using its eigenvectors, was strongly correlated with the structure of the PCA (Appendix S2), and thus we used \mathbf{K} as the sole source of corrections for confounding due to relatedness and population structure when fitting BSLMMs. Estimates of hyperparameters from GEMMA were consistent with the expected polygenic architecture for each phenotypic trait (Table 3). Values of PVE, an approximation of narrow-sense heritability (h^2), ranged from 0.375 (Mass) to 0.514 (LDT). Additionally, the number of SNPs retained in the BLSMM for each phenotypic trait, upon which estimates of PVE are based, ranged from 103 (Mass and PD) to 105 (LDT). However, PIP did not exceed 0.03 for any SNP for any phenotypic trait, which is consistent with different draws from the posterior distribution of BSLMMs for each phenotypic trait containing different sets of SNPs on average, even

TABLE 2 Summary of redundancy analyses (RDAs) examining relationships among phenotypic trait (phen), and genetic (gen) and geographical (geo) data

Model	F (df)	p	R^2	R^2_{adj}
phen ~ geo + gen	2.088 (19,145)	0.001	0.215	0.112
phen ~ gen + Condition(geo)	1.938 (17,145)	0.001	0.178	0.087
phen ~ geo + Condition(gen)	3.331 (2,145)	0.012	0.036	0.028

when the number of SNPs was similar across draws. As such, the estimates of PGE had credible intervals approximately spanning the entire range of the prior distribution and posterior distributions that were relatively flat across the range of the prior distribution (Supporting Information Figures S3 and S4, Appendix S3).

Total effect sizes were on average small (Figure 5), with the absolute value of the mean total effect size per phenotypic trait ranging from 6.27×10^{-5} (Mass) to 8.34×10^{-5} (LDT), and varied across annotation categories (Supporting Information Figure S5). Reported effect sizes, however, were on scale of units of standard deviations in the normal quantile transformed phenotypic trait data. Total effect sizes were moderately correlated across SNPs for LDT and PD (Pearson's $r = -0.462$) and LDT and Mass (Pearson's $r = 0.242$), but only weakly for PD and Mass (Pearson's $r = -0.052$). Absolute effect sizes, including polygenic effects only (α_i) and sparse effects only (β_i), were correlated with PIP values (Pearson's $r > 0.48$), with correlations for sparse effects ($0.48 < \text{Pearson's } r < 0.62$) slightly greater than those for polygenic effects ($0.48 < \text{Pearson's } r < 0.59$). The two components of the total effect size for each SNP (i.e., the polygenic effect [α_i] and the sparse effect [$\beta_i\gamma_i$]) were positively correlated for each phenotypic trait (Mass: Pearson's $r = 0.963$; PD: Pearson's $r = 0.963$; LDT: Pearson's $r = 0.975$). On average, the estimated polygenic effect accounted for 55% (Mass) to 58% (LDT) of the total effect size per SNP for each phenotypic trait. Only 5,992 (LDT) to 7,750 (Mass) SNPs had differences between the sign of their effect for α_i and $\beta_i\gamma_i$. All of these SNPs had effect sizes close to zero.

We defined sets of 86 SNPs associated with each phenotypic trait as those within the lower 0.05% or upper 99.95% tails of the total effect size distribution. Each set of 86 SNPs represented 70 (Mass), 71 (PD) or 69 (LDT) unique contigs in the assembly. Overlap between sets of associated SNPs across phenotypic traits was minimal, with only one (Mass and PD) to five (PD and LDT) associated SNPs shared between phenotypic traits. Associated SNPs had absolute values of their total effect sizes 10.84-fold (Mass) to 14.33-fold (PD) larger than the absolute value of the mean total effect size across all SNPs for each phenotypic trait. Patterns of genetic structure across populations for these sets of SNPs did not differ strongly from the global F_{ST} value (i.e., multilocus F_{ST} ranging from 0.051 [PD] to 0.062 [Mass] relative to the global value of 0.069; Supporting Information Figure S6) nor did the mean absolute value of allele frequency differences across populations (i.e., 0.137 [PD] to 0.147 [Mass] for associated SNPs relative to the global value of 0.124; Supporting Information Figure S7). Patterns of missing data or heterogeneity in estimation across MCMC runs, moreover, did not differentiate associated SNPs (Supporting Information Appendix S4; Figures S8–S10). These sets of SNPs differed relative to randomly selected SNPs, however, in the larger magnitudes of the correlation between allele frequency differences and phenotypic trait differences across populations and the consistency of the sign of this correlation across SNPs (Supporting Information Appendix S5; Figure S11). On average, associated SNPs also had larger contributions of sparse effects to their total effect sizes (63%–70%) relative to all SNPs (55%–58%).

FIGURE 4 Phenotypic trait variation is affected by geography and genetics, as quantified using redundancy analysis (RDA). Shown is the triplot from the full RDA model with sampled moths coloured by populations. Summary statistics of model fit and statistical significance are given in the upper left corner.

Geographical variables are given as black vectors, while genetic variables are given as blue vectors. Phenotypic traits are positioned in red text. The top two RDA axes explained 87.17% of the total effect ($R^2 = 0.215$). Distributions of RDA axis scores by population are given above (Axis 1) and to the right (Axis 2) of the triplot. The results of Kruskal–Wallis tests, which were used to assess differentiation of RDA axis scores by population, are given in each panel

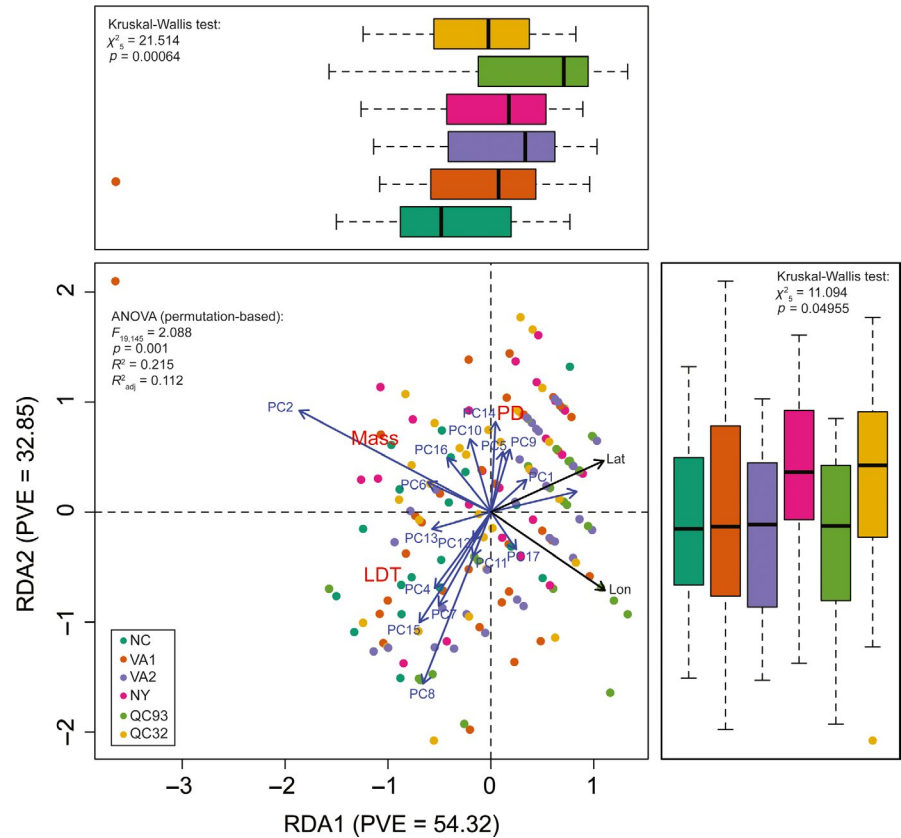


TABLE 3 Combined estimates of hyperparameters describing the architecture of each phenotypic trait are consistent with their expected polygenic bases

Hyperparameter	Mass	PD	LDT
PVE	0.338 (0.076–0.671)	0.387 (0.010–0.766)	0.528 (0.246–0.783)
PGE	0.125 (5.75E-05–0.948)	0.440 (3.15E-04–0.947)	0.066 (6.67E-05–0.945)
N	103 (77–285)	103 (80–289)	105 (78–284)

Shown are approximate maximum a posteriori (MAP) estimates and 95% highest probability densities (HPDs). Estimates for each MCMC run are given in Table S1, with assessment of convergence across runs located in Tables S2 and S3.

3.3 | Evolutionary genetics of associated loci

The aforementioned patterns of associated SNPs suggest coordinated allele frequency shifts across populations contributing to local adaptation. To test this hypothesis explicitly, we used the method of Berg and Coop (2014). All three sets of associated SNPs were consistent with the action of divergent natural selection across populations, with the observed value of the Q_X statistic being larger than expected under a null model of genetic drift for all three phenotypic traits (Figure 5; Table 4). This was most apparent for LDT ($Q_X = 42.561$, $p < 0.0001$) and least apparent for PD ($Q_X = 22.191$, $p = 0.0006$). The driver of this result was the LD component of Q_X , with only this component being statistically significant. This result was not an artefact of physical linkage, as SNPs located on the same contig in the assembly were pruned prior to this analysis. We also

tested the way in which we defined sets of associated SNPs on these results (Supporting Information Appendix S6; Figures S12–S15). The Q_X statistic and both of its components were always larger than those from random sets of SNPs for Mass and LDT (Supporting Information Figures S12 and S13). For PD, however, one of the random sets of SNPs had a larger estimate of Q_X , which was driven by a value of the LD component approximately as large as that listed in Table 4. A similar pattern was observed when more extreme tails of the total effect size distribution were used (Supporting Information Figures S14 and S15). Thus, it appears that LDT and Mass are the two phenotypic traits most consistent with the action of divergent natural selection.

The populations contributing most to this signal of divergent natural selection were the NC and QC93 populations (Table 5). The Z-statistic was statistically significant for NC for all three phenotypic

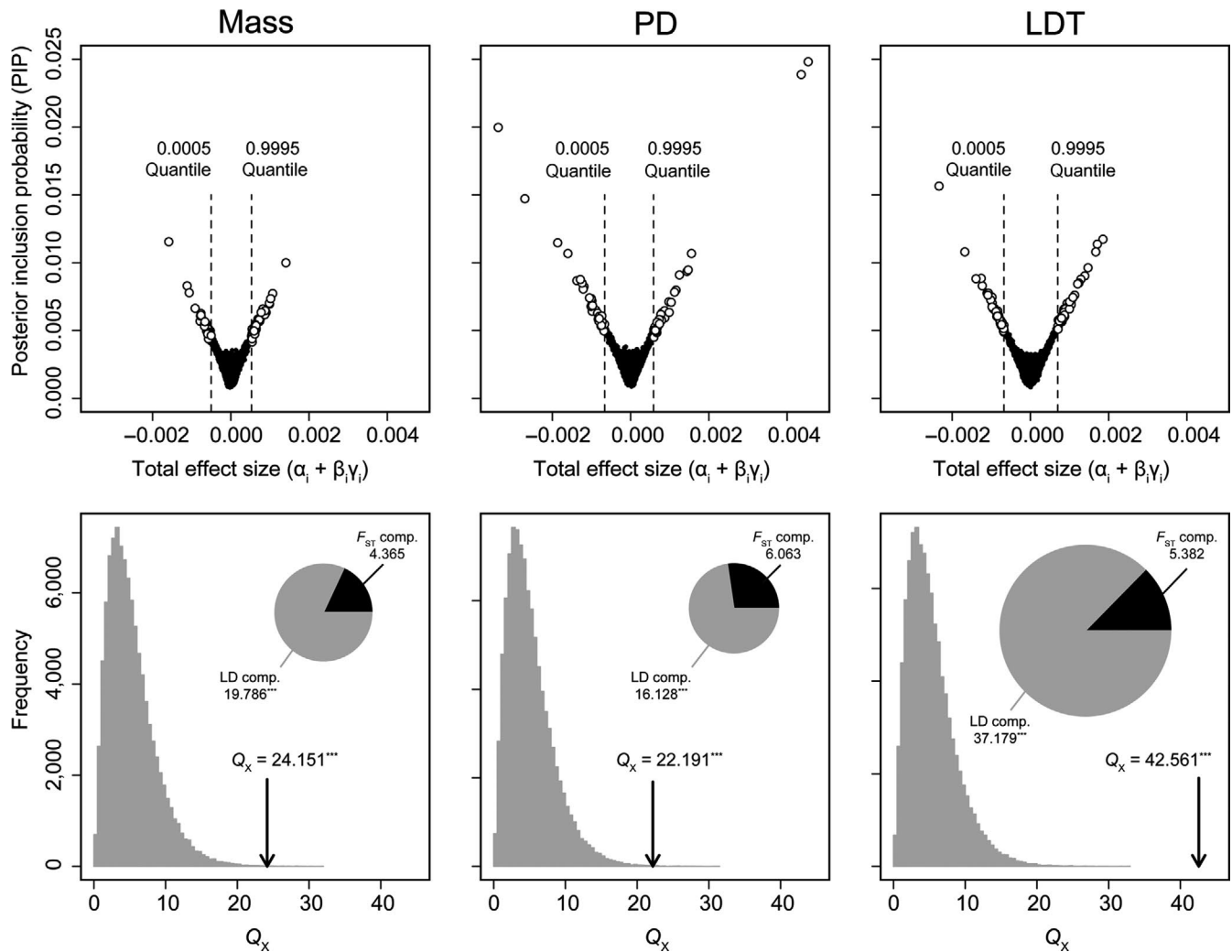


FIGURE 5 Outliers from genome-wide association studies for each trait were identified using the 0.0005 and 0.9995 quantiles (dashed vertical lines) of the total effect size, which were also those SNPs with the largest PIPs (a–c). In all volcano plots, associated loci are identified as open circles. Associated SNPs for each phenotypic trait also had elevated values for the Q_X statistic relative to null distributions (grey histograms), with the LD component accounting for the majority of magnitude for the Q_X statistic (d–f). Inset pie charts are scaled to the maximum value of the Q_X statistic, which was for LDT. * $p < 0.05$, ** $p < 0.005$, *** $p < 0.0005$

TABLE 4 Summaries of statistical tests (Q_X statistic) for divergent natural selection across populations are consistent with linkage disequilibrium (LD) among associated SNPs driving statistically significant, adaptive patterns

Phenotypic trait	F_{ST} (95% CI)	Q_X (p-value)	F_{ST} component (p-value)	LD component (p-value)
Mass ($n = 70$)	0.057 (0.043–0.072)	24.151 (<0.0001)	4.365 (0.9660)	19.786 (<0.0001)
PD ($n = 71$)	0.055 (0.041–0.068)	22.191 (0.0006)	6.063 (0.1476)	16.128 (0.0007)
LDT ($n = 69$)	0.065 (0.051–0.079)	42.561 (<0.0001)	5.382 (0.4250)	37.179 (<0.0001)

Values for F_{ST} are given as the multilocus value calculated from variance components for the SNPs in the associated set for each phenotypic trait. Confidence intervals (CIs) for these multilocus values were generated via bootstrap resampling across SNPs ($n = 1,000$ replicates). The p -values for statistical tests of Q_X and its components were based on null distributions created from resampling unassociated SNPs matched on minor allele frequency (see Materials and Methods). Prior to analysis, the set of associated SNPs for each phenotypic trait was thinned to one SNP per contig in the assembly to avoid physical linkage confounding patterns of LD.

traits and QC93 for Mass and LDT. This was consistent with these populations being the most different in their phenotypic trait distributions for Mass and LDT (Figure 2) and score distributions on RDA axis 1 (Figure 4). Given the values of the Z-statistics for these

populations, as well as the patterns in Figures 2 and 4, divergent natural selection appears to have resulted in larger masses and longer LDT in the NC population and the opposite in the QC93 population. In no case was the observed Z-statistic in the 10 random data sets

more extreme for LDT or Mass in either the NC or the QC93 population (Supporting Information Figures S13 and S15).

4 | DISCUSSION

Rapid adaptation can occur in the presence of strong selection pressures in novel environments (Jain & Stephan, 2017). Here, we demonstrate this using an ecological genomic analysis of gypsy moth populations sampled along a latitudinal transect. Our main conclusion is that populations of gypsy moths at the southern and northern range limits of this species, each established no longer than 30 generations ago (i.e., generation time is 1 year and colonization of these areas is within the last 30 years), are experiencing divergent selection pressures on polygenic traits related to thermal tolerance and that these selection pressures manifest as coordinated allele frequency shifts across populations. Our conclusion was supported by robust signals even in the presence of patterns of missing data, as well as several modelling assumptions.

4.1 | Coordinated allele frequency shifts underlie phenotypic trait differentiation

Evidence for spatially varying or divergent selection acting upon polygenic traits is accumulating for model and nonmodel species (Babin, Gagnaire, Pavey, & Bernatchez, 2017; Berg, Zhang, & Coop, 2017; Crossley et al., 2017; Gagnaire & Gaggiotti, 2016; He et al., 2016; Lind, Menon, Bolte, Fasje, & Eckert, 2018; Pritchard, Pickrell, & Coop, 2010; Rose, Bay, Morikawa, & Palumbi, 2018; Turchin et al., 2012). Here, we explicitly tested for signals of rapid adaptation in novel environments based on coordinated allele frequency shifts within a polygenic architecture across populations of an invasive species. Empirical patterns were consistent with theoretical predictions for strong divergent selection acting on a fitness-related polygenic trait (Chevin & Hospital, 2008; Jain & Stephan, 2015, 2017; Le Corre & Kremer, 2003, 2012; see Supporting Information Table S4). These theoretical expectations are based on several assumptions, so that agreement between data patterns and theoretical predictions

alone is not sufficient for making strong conclusions. Additional evidence justifying the validity of each assumption, however, strengthens and contextualizes our conclusions.

First, selection pressures are assumed to be strong, so that the fitness effects of deviations from local optima are large. Although we did not measure fitness variation directly, the three phenotypic traits we assayed have strong fitness effects when trait values deviate from temperature optima (Honěk, 1993; Logan et al., 1991; Myers et al., 2000). Larval development time and PD are temperature dependent in the gypsy moth (Casagrande, Logan, & Wallner, 1987) and are important phenotypic traits for completing development within the growing season and for synchrony in adult emergence to promote mate-finding (Contarini, Onufrieva, Thorpe, Raffa, & Tobin, 2009; Gray, 2004). Pupal mass is also strongly correlated with fecundity, where increased size results in a larger number of eggs (Calvo & Molina, 2005; Honěk, 1993; Myers et al., 2000). Second, phenotypic optima are assumed to differ across populations, with the relevant importance of coordinated allele frequency shifts increasing as these optima diverge (Le Corre & Kremer, 2003). Previous experimental work supports the idea that temperature optima differ across gypsy moth populations. Caterpillar growth and development are more resilient to high temperatures in southern relative to northern populations (Thompson et al., 2017). Third, phenotypic trait variation is assumed to be determined by numerous small effect loci. If we equate the number of potentially causative loci to the number of SNPs retained in the multi-SNP models constructed in GEMMA (N), which is sensible as the model PVE numerically approximated established heritability estimates for these phenotypic traits, then the number of causative loci for each trait is on the order of at least 100 (Table 3). Note, however, that without full genomic coverage this number is likely to be underestimated. Estimated total effect sizes, moreover, for associated SNPs were small, as assessed in units of trait standard deviations for the normal quantile transformed data, and approximately equally determined by polygenic and sparse effects. Last, levels of gene flow are assumed to be high, so that genetic diversity within populations undergoing strong selection pressures is restored through gene flow among populations with different optima. Historical rates of gypsy moth spread are

TABLE 5 Population-specific tests of adaptive evolution following Berg and Coop (2014) reveal that the strongest signals of divergent natural selection are due to marginal populations located on the northern (QC93) and southern (NC) range margins, especially for LDT and Mass

Population	Mass	PD	LDT
	Z-statistic (<i>p</i> -value)	Z-statistic (<i>p</i> -value)	Z-statistic (<i>p</i> -value)
NC	2.914 (0.0046)	4.289 (0.00004)	5.413 (<0.00001)
VA1	-0.854 (0.402)	0.658 (0.517)	-0.197 (0.804)
VA2	-2.432 (0.018)	-1.887 (0.053)	-1.578 (0.118)
NY	0.559 (0.651)	-0.734 (0.569)	0.013 (0.765)
QC93	-2.749 (0.011)	-0.615 (0.536)	-4.174 (0.00004)
QC32	1.293 (0.187)	-1.601 (0.095)	0.462 (0.724)

The *p*-values were generated from null distributions built from unassociated SNPs matched on minor allele frequency (see Materials and Methods). Results with $p < 0.05$ are in bold type. Prior to analysis, the set of associated SNPs for each phenotypic trait was thinned to one SNP per contig in the assembly to avoid physical linkage confounding patterns of LD.

cyclical and have been well characterized, where low spread rates in the early 20th century align with predications based solely on natural dispersal (~2.5 km/year based on larval ballooning and male flight; Liebhold et al., 1992). However, large-scale expansion at a rate of ~21 km/year began in the mid-1960s, with increased anthropogenic transportation of egg masses implicated as an important source of long-distance dispersal, increased spread rates and probable substantial gene flow among populations (Liebhold, Sharov, & Tobin, 2007; Liebhold & Tobin, 2006). Well-known human vectors for the movement of gypsy moth life stages (e.g., firewood transport, house moves, recreational vehicles) have been correlated with spread rates (Whitmire & Tobin, 2006), so that gene flow among populations is expected to be a common occurrence and is likely to be at reasonably high magnitudes, even at broad spatial scales.

4.2 | Ecophysiological roles of LDT and Mass in environmental adaptation

Much attention has been given to the evolution of geographical patterns in body size (e.g., Blackburn, Gaston, & Loder, 1999, Chown & Gaston, 2010). The most common relationship described is the occurrence of larger body sizes with increasing latitude, although the underlying mechanisms remain of debate (Atkinson & Sibly, 1997). A decrease in body size with latitude, however, has also been documented in several species of insects (Blanckenhorn & Demont, 2004; Chown & Gaston, 1999). This pattern occurs when generation time constitutes a significant portion of the growing season. In this case, season length places constraints on the time and resources available for growth and development and can result in selection for maturation at a smaller body size (Chown & Klok, 2003; Roff, 1980). This is indeed the scenario for the gypsy moth as a univoltine species, where larval and pupal development must be completed in a single growing season and eggs require an obligate overwinter diapause. At the northern range edge, lower temperatures for growth and limitations in season length (Gray, 2004; Tobin, Cremers, Hunt, & Parry, 2016) are probable explanations for selection in the QC93 population for shorter development times and small individuals at maturation. Selection in northern populations for shorter development time based on growing season constraints is also consistent with work showing latitudinal patterns in hatching phenology, where northern populations hatch relatively earlier than southern populations when reared in a common environment, presumably cuing to start the growing season early even at the risk of suboptimal hatching conditions (Śniegula, Gołab, & Johansson, 2016). Similar adjustments to juvenile development in lower temperatures were noted by McEvoy, Higgs, Coombs, Karacetin, and Starcevich (2012) for the cinnabar moth (*Tyria jacobaeae* L.) as it colonized the cooler Cascade Mountains from warmer lowland environments. The lack of such patterns in the QC32 population, however, implies that broad-scale temperature and growing season length alone are not the sole determinants of fitness at the northern range margin (e.g., other climate variables, microclimates). For example, differences in snow cover due to topographical features may interact with temperature

to drive this discrepancy. Future data collected with an appropriate study design, however, would be needed to test this idea rigorously.

Conversely, season length does not place constraints on completing development for southern populations, outside of exposure to supraoptimal temperatures. For insects, increases in size reflected by pupal mass have clear benefits for fecundity, and extending development time provides a longer period for feeding and growth before maturation (Taylor, 1981). At the southern invasion front, the effects from supraoptimal temperatures have been found to be sublethal (Faske et al., 2019) and the amount of heat in a given year is highly variable, resulting in rapid temporal shifts in range dynamics from expansion to contraction (Tobin et al., 2014). While the thermal conditions in this region can be suboptimal, our findings suggest that adaptive changes for increased heat tolerance are occurring with selection for increased development time and size. Indeed, a heat challenge experiment using the same gypsy moth populations found that the NC population had higher survival at a constant supraoptimal rearing temperature as compared to populations QC and NY (see Figures 1 and 2 in Thompson et al., 2017). Mortality events, as evidenced for the gypsy moth by localized range retractions at the southern range front (Tobin et al., 2014), are also indications that selection pressures are strong, which could promote development of locally adapted populations conditional on the availability of adaptive genetic variation (Kuparinen, Savolainen, & Schurr, 2010).

5 | LIMITATIONS AND CONCLUSIONS

Although we assessed the sensitivity of our conclusions to several common concerns about association mapping and selection scans, caution is warranted for several reasons. First, as with all reduced representation methods, only a portion of the genome was interrogated. For genome-wide scans, including any form of association mapping, the degree to which the assayed portion of the genome captures causative segregating variation, directly or through linkage, determines the success of the scan (Lowry et al., 2017a, 2017b). Based on the size of our assembly relative to this expected genome size (750.66 Mb vs. 1.03 Gb, see Petitpierre, 1996), we only interrogated ~20% (i.e., contigs with SNPs covered 26.87% of the length of the full assembly, which covered ~72.88% of the expected size) of the genome for the gypsy moth. The expectation that we missed a portion of relevant variation, however, does not preclude the result that we discovered some of the relevant variation (Catchen et al., 2017; Lowry et al., 2017a, 2017b; McKinney, Larson, Seeb, & Seeb, 2017). For example, some of the annotated genes containing associated SNPs have putative functions with recognized impacts on insect development and physiology during development (Supporting Information Appendix S7; Table S5). Second, we used only a single set of samples to discover and characterize associated SNPs (cf. Berg & Coop, 2014). Although this approach unites estimates of effect sizes for associated SNPs to the samples in which divergent selection is being examined, it could also inflate the prevalence of false positives due to the fact that the SNPs associated with phenotypic

traits already survived corrections for confounding in the GEMMA analysis. The magnitudes of the Q_X statistic for LDT and Mass, however, could not be replicated in the 10 null sets of SNPs selected in similar ways to the associated SNPs. Third, unaccounted for population structure, especially if it is confounded with axes of trait differentiation, could lead to false inference of polygenic selection (Berg et al., 2019). However, neither the magnitudes (i.e., multilocus F_{ST}) nor the patterns of differentiation (i.e., strength of IBD: associated SNPs had Pearson $r^2 = 0.183$ – 0.369 where the genome-wide estimate was $r = 0.459$) were different for associated SNPs relative to genome-wide patterns. Last, weak linkage of our markers with distant, large effect causal sites could appear as a polygenic architecture affected by divergent selection, as signals of association and allele frequency differentiation diminish with the strength of linkage (Bulik-Sullivan et al., 2015; Pritchard & Przeworski, 2001). Using data from contigs with at least two SNPs and fitting pairwise estimates of LD and physical distance to a theoretical expectation (see Hill & Weir, 1988), the rate of decay for LD with physical distance was rapid (Supporting Information Appendix S8; Table S6; Figure S16). Empirical patterns of LD decay, however, were quite variable around their expectations and across populations (Supporting Information Figures S17–S22), so that strong linkage (e.g., $r^2 > 0.90$) was observed at distances up to 10,000 bp. Thus, it is not unreasonable to expect that some of our associated SNPs are not just weakly linked to a handful of large-effect loci.

Regardless of these limitations, our conclusions imply that polygenic adaptation can contribute to range dynamics for invasive species. In the case of gypsy moth, it has long been considered a wide-ranging generalist and few studies have considered the potential for adaptation in range-edge populations. Understanding spread rates and the potential extent of the invasion for the gypsy moth is particularly important because the current range represents approximately only a third of forested habitat susceptible to invasion (McFadden & McManus, 1991). On a more general level, the results here imply that adaptive evolution in novel habitats can occur quickly through coordinated allele frequency shifts from standing genetic variation. How transient are the effects of these coordinated shifts to the overall architecture of local adaptation, however, remains an open question, with answers to this question having implications for the ability of adaptive changes to affect invasion and further spatial spread.

ACKNOWLEDGEMENTS

An award for interdisciplinary research provided from the Thomas F. and Kate Miller Jeffress Memorial Trust funded this work. C.J.F. was supported by the National Science Foundation (NSF) National Plant Genome Initiative (NPGI): Postdoctoral Research Fellowship in Biology (PRFB) FY 2013 Award no. NSF-NPGI-PRFB-1306622. This study was conducted under USDA APHIS permit number P526P-12-01012. We thank the Biology Departments at Virginia Commonwealth University and University of Richmond for providing research facilities and supplies, as well as the VCU Rice Rivers Center

for field space. We would also like to thank the VCU Center for High Performance Computing for computational resources and support. Madison Glackin provided lab support, while Louis Morneau, Rachel Habig and Matt Anderson helped with sample collection.

AUTHOR CONTRIBUTIONS

The research was conceived and designed by K.L.G., D.M.J. and A.J.E. L.M.T., E.M.H., B.M.L., T.M.F., C.J.F., D.P. and K.L.G. generated the data. Computational and statistical analyses were conducted by C.J.F., B.M.L., T.M.F. and A.J.E., with advice and support from R.J.D. A.J.E., T.M.F., C.J.F., L.M.T. and K.L.G. wrote the manuscript. All authors edited and approved the manuscript.

DATA ACCESSIBILITY

Raw sequence data are available at the NCBI short read archive for the ddRADseq data (PRJNA515971), as well as the data used for creation of a reference assembly (PRJNA523392). Genotype calls, phenotypic data, reference contigs, annotations, sampling localities, intermediate data summaries and R scripts used for analysis are available at the Dryad digital repository (<https://doi.org/10.5061/dryad.8ts2867>).

ORCID

Brandon M. Lind  <https://orcid.org/0000-0002-8560-5417>

Andrew J. Eckert  <https://orcid.org/0000-0002-6522-2646>

REFERENCES

- Allendorf, F. E., & Lundquist, L. L. (2003). Introduction: Population biology, evolution, and control of invasive species. *Conservation Biology*, 17, 24–30. <https://doi.org/10.1046/j.1523-1739.2003.02365.x>
- Atkinson, D., & Sibly, R. M. (1997). Why are organisms usually bigger in colder environments? Making sense of a life history puzzle. *Trends in Ecology & Evolution*, 12, 235–239. [https://doi.org/10.1016/S0169-5347\(97\)01058-6](https://doi.org/10.1016/S0169-5347(97)01058-6)
- Babin, C., Gagnaire, P.-A., Pavey, S. A., & Bernatchez, L. (2017). RAD-seq reveals patterns of additive polygenic variation caused by spatially-varying selection in the American eel (*Anguilla rostrata*). *Genome Biology and Evolution*, 9, 2974–2986. <https://doi.org/10.1093/gbe/evx226>
- Baker, H. G., & Stebbins, G. L. (1965). *The genetics of colonizing species*. New York, NY: Academic Press.
- Barrett, R. D., & Schluter, D. (2008). Adaptation from standing genetic variation. *Trends in Ecology and Evolution*, 23, 38–44. <https://doi.org/10.1016/j.tree.2007.09.008>
- Bates, D., Mächler, M. M., Bolker, B., & Walker, S. (2015). Fitting linear mixed-effect models using lme4. *Journal of Statistical Software*, 67, 1–48. <https://doi.org/10.18637/jss.v067.i01>
- Berg, J. J., & Coop, B. C. (2014). A population genetic signal of polygenic adaptation. *PLoS Genetics*, 10, e1004412. <https://doi.org/10.1371/journal.pgen.1004412>
- Berg, J. J., Zhang, X., & Coop, G. (2017). Polygenic adaptation has impacted multiple anthropometric traits. *bioRxiv*. <https://doi.org/10.1101/167551>

- Berg, J. J., Harpak, A., Sinnott-Armstrong, N., Jorgensen, A. M., Mostafavi, H., Field, Y., ... Coop, G. (2019). Reduced signal for polygenic adaptation of height in UK Biobank. *eLife*, 8, e39725. <https://doi.org/10.7554/eLife.39725>
- Blackburn, T. M., Gaston, K. J., & Loder, N. (1999). Geographic gradients in body size: A clarification of Bergmann's rule. *Diversity and Distributions*, 5, 165–174. <https://doi.org/10.1046/j.1472-4642.1999.00046.x>
- Blanckenhorn, W. U., & Demont, M. (2004). Bergmann and converse Bergmann latitudinal clines in arthropods: Two ends of a continuum? *Integrative and Comparative Biology*, 44, 413–424. <https://doi.org/10.1093/icb/44.6.413>
- Blows, M. W., & Hoffmann, A. A. (1993). The genetics of central and marginal populations of *Drosophila serrata*. I. Genetic variation for stress resistance and species borders. *Evolution*, 47, 1255–1270. <https://doi.org/10.1111/j.1558-5646.1993.tb02151.x>
- Bogdanowicz, S. M., Mastro, V. C., Prasher, D. C., & Harrison, R. G. (1997). Microsatellite DNA variation among Asian and North American gypsy moths (Lepidoptera: Lymantriidae). *Annals of the Entomological Society of America*, 90, 768–775. <https://doi.org/10.1093/aesa/90.6.768>
- Borcard, D., Legendre, P., & Drapeau, P. (1992). Partialling out the spatial component of ecological variation. *Ecology*, 73, 1045–1055. <https://doi.org/10.2307/1940179>
- Bulik-Sullivan, B., Finucane, H. K., Anttila, V., Gusev, A., Day, F. R., Loh, P.-R., ... Neale, B. M. (2015). An atlas of genetic correlations across human diseases and traits. *Nature Genetics*, 47, 1236–1241. <https://doi.org/10.1038/ng.3406>
- Caley, M. J., Cripps, E., & Game, E. T. (2013). Phenotypic covariance at species' borders. *BMC Evolutionary Biology*, 13, 105. <https://doi.org/10.1186/1471-2148-13-105>
- Calvo, D., & Molina, J. M. (2005). Fecundity-body size relationship and other reproductive aspects of *Streblothe panda* (Lepidoptera: Lasiocampidae). *Annals of the Entomological Society of America*, 98, 191–196. [https://doi.org/10.1603/0013-8746\(2005\)098\[0191:FSRAOR\]2.0.CO;2](https://doi.org/10.1603/0013-8746(2005)098[0191:FSRAOR]2.0.CO;2)
- Camacho, C., Coulouris, G., Avagyan, V., Ma, N., Papadopoulos, J., Bealer, K., & Madden, T. L. (2009). BLAST+: Architecture and applications. *BMC Bioinformatics*, 10, 421. <https://doi.org/10.1186/1471-2105-10-421>
- Campbell, M. S., Holt, C., Moore, B., & Yandell, M. (2014). Genome annotation and curation using MAKER and MAKER-P. *Current Protocols in Bioinformatics*, 48, 4.11.1–4.11.39. <https://doi.org/10.1002/0471250953.bi0411s48>
- Cantarel, B. L., Korf, I., Robb, S. M. C., Parra, G., Ross, E., Moore, B., ... Yandell, M. (2008). MAKER: An easy-to-use annotation pipeline designed for emerging model organism genomes. *Genome Research*, 18, 188–196.
- Casagrande, R. A., Logan, P. A., & Wallner, W. E. (1987). Phenological model for gypsy moth, *Lymantria dispar* (Lepidoptera: Lymantriidae), larvae and pupae. *Environmental Entomology*, 16, 556–562. <https://doi.org/10.1093/ee/16.2.556>
- Catchen, J. M., Hohenlohe, P. A., Bernatchez, L., Funk, W. C., Andrews, K. R., & Allendorf, F. W. (2017). Unbroken: RADseq remains a powerful tool for understanding the genetics of adaptation in natural populations. *Molecular Ecology Resources*, 17, 362–365. <https://doi.org/10.1111/1755-0998.12669>
- Chevin, L.-M., & Hospital, F. (2008). Selective sweep at a quantitative trait locus in the presence of background genetic variation. *Genetics*, 180, 1645–1660. <https://doi.org/10.1534/genetics.108.093351>
- Chown, S. L., & Klok, C. J. (2003). Altitudinal body size clines: Latitudinal effects associated with changing seasonality. *Ecography*, 26, 445–455. <https://doi.org/10.1034/j.1600-0587.2003.03479.x>
- Chown, S. L., & Gaston, K. J. (1999). Exploring links between physiology and ecology at macro-scales: The role of respiratory metabolism in insects. *Biological Reviews*, 74, 87–120. <https://doi.org/10.1111/j.1469-185X.1999.tb00182.x>
- Chown, S. L., & Gaston, K. J. (2010). Body size variation in insects: A macroecological perspective. *Biological Reviews*, 85, 139–169. <https://doi.org/10.1111/j.1469-185X.2009.00097.x>
- Cock, P. A., Antao, T., Chang, J. T., Chapman, B. A., Cox, C. J., Dalke, A., ... de Hoon, M. J. L. (2009). Biopython: Freely available Python tools for computational molecular biology and bioinformatics. *Bioinformatics*, 25, 1422–1423. <https://doi.org/10.1093/bioinformatics/btp163>
- Contarini, M., Onufrieva, K. S., Thorpe, K. W., Raffa, K. F., & Tobin, P. C. (2009). Mate-finding failure as an important cause of Allee effects along the leading edge of an invading insect population. *Entomologia Experimentalis Et Applicata*, 133, 307–314. <https://doi.org/10.1111/j.1570-7458.2009.00930.x>
- Cook, L. M., & Saccheri, I. J. (2013). The peppered moth and industrial melanism: Evolution of a natural selection case study. *Heredity*, 110, 207–212. <https://doi.org/10.1038/hdy.2012.92>
- Coulatti, R. I., & Lau, J. A. (2015). Contemporary evolution during invasion: Evidence for differentiation, natural selection, and local adaptation. *Molecular Ecology*, 24, 1999–2017. <https://doi.org/10.1111/mec.13162>
- Crossley, M. S., Chen, Y. H., Groves, R. L., & Schoville, S. D. (2017). Landscape genomics of Colorado potato beetle provides evidence of polygenic adaptation to insecticides. *Molecular Ecology*, 26, 6284–6300. <https://doi.org/10.1111/mec.14339>
- Danecek, P., Auton, A., Abecasis, G., Albers, C. A., Banks, E., & DePristo, M. A., ... 1000 Genomes Project Analysis Group (2011). The variant call format and VCFtools. *Bioinformatics*, 27, 2156–2158. <https://doi.org/10.1093/bioinformatics/btr330>
- Dlugosch, K. M., & Parker, I. M. (2008). Founding events in species invasions: Genetic variation, adaptive evolution, and the role of multiple introductions. *Molecular Ecology*, 17, 431–449. <https://doi.org/10.1111/j.1365-294X.2007.03538.x>
- Dlugosch, K. M., Anderson, S. R., Braasch, J., Cang, F. A., & Gillette, H. D. (2015). The devil is in the details: Genetic variation in introduced populations and its contributions to invasion. *Molecular Ecology*, 24, 2095–2111. <https://doi.org/10.1111/mec.13183>
- Eckert, C. G., Samis, K. E., & Loughheed, S. C. (2008). Genetic variation across species' geographical ranges: The central-marginal hypothesis and beyond. *Molecular Ecology*, 17, 1170–1188. <https://doi.org/10.1111/j.1365-294X.2007.03659.x>
- Estoup, A., Ravné, V., Hufbauer, R., Vitalis, R., Gautier, M., & Facon, B. (2016). Is there a genetic paradox of biological invasion? *Annual Review of Ecology, Evolution, and Systematics*, 47, 51–72. <https://doi.org/10.1146/annurev-ecolsys-121415-032116>
- Fält-Nardmann, J. J. J., Ruohomäki, K., Tikkanen, O.-P., & Neuvonen, S. (2018). Cold hardiness of *Lymantria monacha* and *L. dispar* (Lepidoptera: Erebididae) eggs to extreme winter temperatures: Implications for predicting climate change impacts. *Ecological Entomology*, 43, 422–430. <https://doi.org/10.1111/een.12515>
- Fält-Nardmann, J. J. J., Klemola, T., Ruohomäki, K., Niemelä, P., Roth, M., & Saikkonen, K. (2018). Local adaptations and phenotypic plasticity may render gypsy moth and nun moth future pests in northern European boreal forests. *Canadian Journal of Forest Research*, 48, 265–276. <https://doi.org/10.1139/cjfr-2016-0481>
- Faske, T. M., Thompson, L. M., Banahene, N., Levorse, A., Quiroga-Herrera, M., Sherman, K., ... Grayson, K. L. (2019). Can gypsy moth stand the heat? A reciprocal transplant experiment with an invasive forest pest across its southern range margin. *Biological Invasions*, 21, 1365–1378. <https://doi.org/10.1007/s10530-018-1907-9>
- Gagnaire, P.-A., & Gaggiotti, O. E. (2016). Detecting polygenic selection in marine populations by combining population genomics and quantitative genetics approaches. *Current Zoology*, 62, 603–616. <https://doi.org/10.1093/cz/zow088>
- Grant, B. R., & Grant, P. R. (2008). Fission and fusion of Darwin's finches populations. *Philosophical Transactions of the Royal Society B: Biological Sciences*, 363, 2821–2829. <https://doi.org/10.1098/rstb.2008.0051>

- Gray, D. R. (2004). The gypsy moth life stage model: Landscape-wide estimates of gypsy moth establishment using a multi-generational phenology model. *Ecological Modelling*, 176, 155–171. <https://doi.org/10.1016/j.ecolmodel.2003.11.010>
- Grayson, K. L., & Johnson, D. M. (2017). Novel insights on population and range edge dynamics using an unparalleled spatiotemporal record of species invasion. *Journal of Animal Ecology*, 87, 581–593. <https://doi.org/10.1111/1365-2656.12755>
- Guo, Q. (2014). Central-marginal population dynamics in species invasions. *Frontiers in Ecology and Evolution*, 2, 23. <https://doi.org/10.3389/fevo.2014.00023>
- Gurevich, A., Saveliev, V., Vyahhi, N., & Tesler, G. (2013). QUAST: Quality assessment tool for genome assemblies. *Bioinformatics*, 29, 1072–1075. <https://doi.org/10.1093/bioinformatics/btt086>
- He, F., Arce, A. L., Schmitz, G., Koornneef, M., Novikova, P., Beyer, A., & de Meaux, J. (2016). The footprint of polygenic adaptation on stress responsive cis-regulatory divergence in the *Arabidopsis* genus. *Molecular Biology & Evolution*, 33, 2088–2101. <https://doi.org/10.1093/molbev/msw096>
- Hermisson, J., & Pennings, J. S. (2005). Soft sweeps: Molecular population genetics of adaptation from standing genetic variation. *Genetics*, 169, 2335–2352. <https://doi.org/10.1534/genetics.104.036947>
- Hermisson, J., & Pennings, J. S. (2017). Soft sweeps and beyond: Understanding the patterns and probabilities of selection footprints under rapid adaptation. *Methods in Ecology and Evolution*, 8, 700–716. <https://doi.org/10.1111/2041-210X.12808>
- Herten, K., Hestand, M. S., Vermeesch, J. R., & Houdt, J. K. V. (2015). GBSX: A toolkit for experimental design and demultiplexing genotyping by sequencing experiments. *BMC Bioinformatics*, 16, 73. <https://doi.org/10.1186/s12859-015-0514-3>
- Hill, J. K., Griffiths, H. M., & Thomas, C. D. (2011). Climate change and evolutionary adaptations at species' range margins. *Annual Review of Entomology*, 56, 143–159. <https://doi.org/10.1146/annurev-ento-120709-144746>
- Hill, W. G., & Weir, B. S. (1988). Variances and covariances of squared linkage disequilibria in finite populations. *Theoretical Population Biology*, 33, 54–78. [https://doi.org/10.1016/0040-5809\(88\)90004-4](https://doi.org/10.1016/0040-5809(88)90004-4)
- Honěk, A., & Honek, A. (1993). Intraspecific variation in body size and fecundity in insects: A general relationship. *Oikos*, 66, 483–492. <https://doi.org/10.2307/3544943>
- Jain, K., & Stephan, W. (2015). Response of polygenic traits under stabilizing selection and mutation when loci have unequal effects. *G3*, 5, 1065–1074. <https://doi.org/10.1534/g3.115.017970>
- Jain, K., & Stephan, W. (2017). Rapid adaptation of a polygenic trait after a sudden environmental shift. *Genetics*, 206, 389–406. <https://doi.org/10.1534/genetics.116.196972>
- Janković-Tomanić, M., & Lazarević, J. (2012). Effects of temperature and dietary nitrogen on genetic variation and covariation in gypsy moth larvae performance traits. *Archives of Biological Science, Belgrade*, 64, 1109–1116.
- Keller, S. R., & Taylor, D. R. (2008). History, chance and adaptation during biological invasion: Separating stochastic phenotypic evolution from response to selection. *Ecology Letters*, 11, 852–866. <https://doi.org/10.1111/j.1461-0248.2008.01188.x>
- Keller, S. R., Chhatre, V. E., & Fitzpatrick, M. C. (2017). Influence of range position on locally adaptive gene-environment associations in *Populus* flowering time genes. *Journal of Heredity*, 109, 47–58. <https://doi.org/10.1093/jhered/esx098>
- Kingsolver, J. G., & Woods, H. A. (1997). Thermal sensitivity of growth and feeding in *Manduca sexta* caterpillars. *Physiological Zoology*, 70, 631–638. <https://doi.org/10.1086/515872>
- Korf, I. (2004). Gene finding in novel genomes. *BMC Bioinformatics*, 5, 59. <https://doi.org/10.1186/1471-2105-5-59>
- Kunin, W. E., Vergeer, P., Kenta, T., Davey, M. P., Burke, T., Woodward, F. I., ... Butlin, R. (2009). Variation at range margins across multiple spatial scales: Environmental temperature, population genetics and metabolomics phenotype. *Proceedings of the Royal Society B: Biological Sciences*, 276, 1495–1506. <https://doi.org/10.1098/rspb.2008.1767>
- Kuparinen, A., Savolainen, O., & Schurr, F. M. (2010). Increased mortality can promote evolutionary adaptation of forest trees to climate change. *Forest Ecology and Management*, 259, 1003–1008. <https://doi.org/10.1016/j.foreco.2009.12.006>
- Lamichaney, S., Berglund, J., Sällman Almén, M., Maqbool, K., Grabherr, M., Martinez-Barrio, A., ... Andersson, L. (2015). Evolution of Darwin's finches and their beaks revealed by genome sequencing. *Nature*, 518, 371–375. <https://doi.org/10.1038/nature14181>
- Langmead, B., & Salzberg, S. L. (2012). Fast gapped-read alignment with Bowtie 2. *Nature Methods*, 9, 357–359. <https://doi.org/10.1038/nmeth.1923>
- Lazarević, J., Perić-Mataruga, V., Ivanović, J., & Anđelković, M. (1998). Host plant effects on the genetic variation and correlations in the individual performance of the gypsy moth. *Functional Ecology*, 12, 141–148. <https://doi.org/10.1046/j.1365-2435.1998.00166.x>
- Lazarević, J., Perić-Mataruga, V., Stojković, B., & Tucić, N. (2002). Adaptation of the gypsy moth to an unsuitable host plant. *Entomologia Experimentalis Et Applicata*, 102, 75–86. <https://doi.org/10.1046/j.1570-7458.2002.00926.x>
- Lazarević, J., Perić-Mataruga, V., & Tucić, N. (2007). Pre-adult development and longevity in natural populations of *Lymantria dispar* (Lepidoptera: Lymantriidae). *European Journal of Entomology*, 104, 211–216. <https://doi.org/10.14411/eje.2007.033>
- Lazarević, J., Nenadović, V., Janković-Tomanić, M., & Milanović, S. (2008). Genetic variation and correlations of life-history traits in gypsy moths (*Lymantria dispar* L.) from two populations in Serbia. *Archives of Biological Science, Belgrade*, 60, 619–627. <https://doi.org/10.2298/ABS0804619L>
- Le Corre, V., & Kremer, A. (2003). Genetic variability at neutral markers, quantitative trait loci and trait in a subdivided population under selection. *Genetics*, 164, 1205–1219.
- Le Corre, V., & Kremer, A. (2012). The genetic differentiation at quantitative trait loci under local adaptation. *Molecular Ecology*, 21, 1548–1566. <https://doi.org/10.1111/j.1365-294X.2012.05479.x>
- Legendre, P., & Legendre, L. (2012). *Numerical ecology*. 3rd ed. Oxford, UK: Elsevier.
- Legendre, P., Fortin, M.-J., & Borcard, D. (2015). Should the Mantel test be used in spatial analysis? *Methods in Ecology and Evolution*, 6, 1239–1247. <https://doi.org/10.1111/2041-210X.12425>
- Li, H., Handsaker, B., Wysoker, A., Fennell, T., Ruan, J., & Homer, N., ... 1000 Genome Project Data Processing Subgroup (2009). The Sequence Alignment/Map format and SAMtools. *Bioinformatics*, 25, 2078–2079. <https://doi.org/10.1093/bioinformatics/btp352>
- Liebold, A., Mastro, V., & Schaefer, P. W. (1989). Learning from the legacy of Leopold Trouvelot. *Bulletin of the Entomological Society of America*, 35, 20–22. <https://doi.org/10.1093/besa/35.2.20>
- Liebold, A. M., Halverson, J. A., & Elmes, G. A. (1992). Gypsy moth invasion in North America: A quantitative analysis. *Journal of Biogeography*, 19, 513–520. <https://doi.org/10.2307/2845770>
- Liebold, A. M., & Tobin, P. C. (2006). Growth of newly established alien populations: Comparison of North American gypsy moth colonies with invasion theory. *Population Ecology*, 48, 253–262. <https://doi.org/10.1007/s10144-006-0014-4>
- Liebold, A. M., Sharov, A. A., & Tobin, P. C. (2007). Population biology of gypsy moth spread. In P. C. Tobin, & L. M. Blackburn (Eds.), *Slow the spread: A national program to manage the gypsy moth* (pp. 15–32). General Technical Report NRS-6. Newtown Square, PA: USDA-Forest Service.
- Limbau, S., Kenna, M., Chen, F., Cook, G., Nadel, H., & Hoover, K. (2017). Effects of temperature on development of *Lymantria dispar asiatica* and *Lymantria dispar japonica* (Lepidoptera: Erebididae). *Environmental Entomology*, 46, 1012–1023. <https://doi.org/10.1093/ee/nvx111>

- Lind, B. M., Menon, M., Bolte, C. E., Faske, T. M., & Eckert, A. J. (2018). The genomics of local adaptation in trees: Are we out of the woods yet? *Tree Genetics and Genomes*, *14*, 29. <https://doi.org/10.1007/s11295-017-1224-y>
- Logan, J. A., Casagrande, R. A., & Liebhold, A. M. (1991). Modeling environment for simulation of gypsy moth (Lepidoptera: Lymantriidae) larval phenology. *Environmental Entomology*, *20*, 1516–1525. <https://doi.org/10.1093/ee/20.6.1516>
- Lohmueller, K. E., Indap, A. R., Schmidt, S., Boyko, A. R., Hernandez, R. D., Hubisz, M. J., ... Bustamante, C. D. (2008). Proportionally more deleterious genetic variation in European than in African populations. *Nature*, *451*, 994–997. <https://doi.org/10.1038/nature06611>
- Lowe, T. M., & Eddy, S. R. (1997). tRNAscan-SE: A program for improved detection of transfer RNA genes in genomic sequence. *Nucleic Acids Research*, *25*, 955–964. <https://doi.org/10.1093/nar/25.5.955>
- Lowry, D. B., Hoban, S., Kelley, J. L., Lotterhos, K. E., Reed, L. K., Antolin, M. F., & Storer, A. (2017a). Breaking RAD: An evaluation of the utility of restriction site-associated DNA sequencing for genome scans of adaptation. *Molecular Ecology Resources*, *17*, 142–152. <https://doi.org/10.1111/1755-0998.12635>
- Lowry, D. B., Hoban, S., Kelley, J. L., Lotterhos, K. E., Reed, L. K., Antolin, M. F., & Storer, A. (2017b). Responsible RAD: Striving for best practices in population genomic studies of adaptation. *Molecular Ecology Resources*, *17*, 366–369. <https://doi.org/10.1111/1755-0998.12677>
- Luikart, G., Allendorf, F. W., Cornuet, J. M., & Sherwin, W. B. (1998). Distortion of allele frequency distributions provides a test for recent population bottlenecks. *Journal of Heredity*, *89*, 238–247. <https://doi.org/10.1093/jhered/89.3.238>
- McEvoy, P. B., Higgs, K. M., Coombs, E. M., Karacetin, E., & Starcevic, L. A. (2012). Evolving while invading: Rapid adaptive evolution in juvenile development time for a biological control organism colonizing a high-elevation environment. *Evolutionary Applications*, *5*, 524–536. <https://doi.org/10.1111/j.1752-4571.2012.00278.x>
- McFadden, M. W., & McManus, M. E. (1991). An insect out of control? The potential for spread and establishment of the gypsy moth in new forest areas in the United States. In Y. N. Baranchikov, W. J. Mattson, F. P. Hain, & T. L. Payne (Eds.), *Forest insect guilds: Patterns of interaction with host trees* (pp. 172–186). General Technical Report NE-153. Abakan, Siberia: USDA-Forest Service Northern Research Station.
- McKinney, G. J., Larson, W. A., Seeb, L. W., & Seeb, J. E. (2017). RADseq provides unprecedented insights into molecular ecology and evolutionary genetics: Comment on Breaking RAD by Lowry et al. (2016). *Molecular Ecology Resources*, *17*, 356–361. <https://doi.org/10.1111/1755-0998.12649>
- Myers, J. H., Malakar, R., & Cory, J. S. (2000). Sublethal nucleopolyhedrovirus infection effects on female pupal weight, egg mass size, and vertical transmission in gypsy moth (Lepidoptera: Lymantriidae). *Environmental Entomology*, *29*, 1268–1272. <https://doi.org/10.1603/0046-225X-29.6.1268>
- Oksanen, J., Blanchet, F. G., Friendly, M., Kindt, R., Legendre, P., McGinn, D., ... Wagner, H. (2017). *vegan: Community ecology package. R package ver. 2.4-3*. Retrieved from <https://CRAN.R-project.org/package=vegan>
- Orr, H. A. (2005). The genetic theory of adaptation: A brief history. *Nature Reviews Genetics*, *6*, 119–127. <https://doi.org/10.1038/nrg1523>
- Paccard, A., Van Buskirk, J., & Willi, Y. (2016). Quantitative genetic architecture at latitudinal range boundaries: Reduced variation but higher trait independence. *The American Naturalist*, *187*, 667–677. <https://doi.org/10.1086/685643>
- Páez, D. J., Fleming-Davies, A. E., & Dwyer, G. (2015). Effects of pathogen exposure on life-history variation in the gypsy moth (*Lymantria dispar*). *Journal of Evolutionary Biology*, *28*, 1828–1839. <https://doi.org/10.1111/jeb.12699>
- Parchman, T. L., Gompert, Z., Mudge, J., Schilkey, F. D., Benkman, C. W., & Buerkle, C. A. (2012). Genome-wide association genetics of an adaptive trait in lodgepole pine. *Molecular Ecology*, *21*, 2991–3005. <https://doi.org/10.1111/j.1365-294X.2012.05513.x>
- Patterson, N., Price, A. L., & Reich, D. (2006). Population structure and eigenanalysis. *PLoS Genetics*, *2*, e190. <https://doi.org/10.1371/journal.pgen.0020190>
- Pérez, F., & Granger, B. E. (2007). IPython: A system for interactive scientific computing. *Computing in Science and Engineering*, *9*, 21–29. <https://doi.org/10.1109/MCSE.2007.53>
- Petitpierre, E. (1996). Molecular cytogenetics and taxonomy of insects, with particular reference to the coleoptera. *International Journal of Insect Morphology and Embryology*, *25*, 115–133. [https://doi.org/10.1016/0020-7322\(95\)00024-0](https://doi.org/10.1016/0020-7322(95)00024-0)
- Picq, S., Keena, M., Havill, N., Stewart, D., Pouliot, E., Boyle, B., ... Cusson, M. (2018). Assessing the potential of genotyping-by-sequencing-derived single nucleotide polymorphisms to identify the geographic origins of intercepted gypsy moth (*Lymantria dispar*) specimens: A proof-of-concept study. *Evolutionary Applications*, *11*, 325–339. <https://doi.org/10.1111/eva.12559>
- Plummer, M., Best, N., Cowles, K., & Vines, K. (2006). CODA: Convergence diagnosis and output analysis for MCMC. *R News*, *6*, 7–11.
- Pritchard, J. K., & Przeworski, M. (2001). Linkage disequilibrium in humans: Models and data. *American Journal of Human Genetics*, *69*, 1–14. <https://doi.org/10.1086/321275>
- Pritchard, J. K., & Di Rienzo, A. (2010). Adaptation – Not by sweeps alone. *Nature Reviews Genetics*, *11*, 665–667. <https://doi.org/10.1038/nrg2880>
- Pritchard, J. K., Pickrell, J. K., & Coop, G. (2010). The genetics of human adaptation: Hard sweeps, soft sweeps, and polygenic adaptation. *Current Biology*, *20*, R208–R215. <https://doi.org/10.1016/j.cub.2009.11.055>
- R Core Team (2017). *R: A language and environment for statistical computing*. Vienna, Austria: R Foundation for Statistical Computing. <https://www.R-project.org/>
- Rehm, E. M., Olivias, P., Stroud, J., & Feeley, K. J. (2015). Losing your edge: Climate change and the conservation value of range-edge populations. *Ecology and Evolution*, *5*, 4315–4326. <https://doi.org/10.1002/ece3.1645>
- Roff, D. A. (1980). Optimizing development time in a seasonal environment: The “ups and downs” of clinal variation. *Oecologia*, *45*, 202–208. <https://doi.org/10.1007/BF00346461>
- Rose, N. H., Bay, R. A., Morikawa, M. K., & Palumbi, S. R. (2018). Polygenic evolution drives species divergence and climate adaptation in corals. *Evolution*, *72*, 82–94. <https://doi.org/10.1111/evo.13385>
- Rossiter, M. C. (1991). Environmentally-based maternal effects: A hidden force in insect population dynamics? *Oecologia*, *87*, 288–294. <https://doi.org/10.1007/BF00325268>
- Sagarin, R. D., Gaines, S. D., & Gaylord, B. (2006). Moving beyond assumptions to understand abundance distributions across the ranges of species. *Trends in Ecology & Evolution*, *21*, 524–530. <https://doi.org/10.1016/j.tree.2006.06.008>
- Sharov, A. A., Leonard, D., Liebhold, A. M., Roberts, E. A., & Dickerson, W. (2002). “Slow the Spread” – A national program to contain the gypsy moth. *Journal of Forestry*, *100*, 30–35.
- Simão, F. A., Waterhouse, R. M., Ioannidis, P., Kriventseva, E. V., & Zdobnov, E. M. (2015). BUSCO: Assessing genome assembly and annotation completeness with single-copy orthologs. *Bioinformatics*, *31*, 3210–3212. <https://doi.org/10.1093/bioinformatics/btv351>
- Slater, G. S., & Birney, E. (2005). Automated generation of heuristics for biological sequence comparison. *BMC Bioinformatics*, *6*, 31. <https://doi.org/10.1186/1471-2105-6-31>
- Smit, A. F. A., Hubley, R., & Green, P. (2015). *RepeatMasker Open-4.0*. 2013–2015. Retrieved from <http://www.repeatmasker.org>
- Śniegula, S., Gołab, M. J., & Johansson, F. (2016). Time constraint effects on phenology and life history synchrony in a damselfly along a latitudinal gradient. *Oikos*, *125*, 414–423. <https://doi.org/10.1111/oik.02265>

- Stanke, M., & Waack, S. (2003). Gene prediction with a hidden-Markov model and a new intron Submodel. *Bioinformatics*, *19*(Suppl. 2), ii215–ii225.
- Stanke, M., Steinkamp, R., Waack, S., & Morgenstern, B. (2004). AUGUSTUS: A web server for gene finding in eukaryotes. *Nucleic Acids Research*, *32*, W309–W312. <https://doi.org/10.1093/nar/gkh379>
- Suarez, A. V., & Tsutsui, N. D. (2008). The evolutionary consequences of biological invasions. *Molecular Ecology*, *17*, 351–360. <https://doi.org/10.1111/j.1365-294X.2007.03456.x>
- Taylor, F. (1981). Ecology and evolution of physiological time in insects. *The American Naturalist*, *117*, 1–23. <https://doi.org/10.1086/283683>
- Ter-Hovhannisyanyan, V., Lomsadze, A., Chernoff, Y. O., & Borodovsky, M. (2008). Gene prediction in novel fungal genomes using an *ab initio* algorithm with unsupervised training. *Genome Research*, *18*, 1979–1990. <https://doi.org/10.1101/gr.081612>
- Therry, L., Nilsson-Örtman, V., Bonte, D., & Stoks, R. (2014). Rapid evolution of larval life history, adult immune function and flight muscles in a poleward-moving damselfly. *Journal of Evolutionary Biology*, *27*, 141–152. <https://doi.org/10.1111/jeb.12281>
- Thompson, L. M., Faske, T. M., Banahene, N., Grim, D., Agosta, S. J., Parry, D., ... Grayson, K. L. (2017). Variation in growth and developmental responses to supraoptimal temperatures near latitudinal range limits of gypsy moth *Lymantria dispar* (L.), an expanding invasive species. *Physiological Entomology*, *42*, 181–190. <https://doi.org/10.1111/phen.12190>
- Tobin, P. C., Bai, B. B., Eggen, D. A., & Leonard, D. S. (2012). The ecology, geopolitics, and economics of managing *Lymantria dispar* in the United States. *International Journal of Pest Management*, *58*, 195–210.
- Tobin, P. C., Gray, D. R., & Liebhold, A. M. (2014). Supraoptimal temperatures influence the range dynamics of a non-native insect. *Diversity and Distributions*, *20*, 813–823. <https://doi.org/10.1111/ddi.12197>
- Tobin, P. C., Cremers, K. T., Hunt, L., & Parry, D. (2016). All quiet on the western front? Using phenological inference to detect the presence of a latent gypsy moth invasion in Northern Minnesota. *Biological Invasions*, *18*, 3561–3573. <https://doi.org/10.1007/s10530-016-1248-5>
- Turchin, M. C., Chiang, C. W., Palmer, C. D., Sankararaman, S., Reich, D., ... Hirschhorn, J. N. (2012). Evidence of widespread selection on standing variation in Europe at height-associated SNPs. *Nature Genetics*, *44*, 1015–1019. <https://doi.org/10.1038/ng.2368>
- van't Hof, A. E., Edmonds, N., Dalikova, M., Marec, F., & Saccheri, I. J. (2011). Industrial melanism in British peppered moths has a singular and recent mutational origin. *Science*, *332*, 958–960. <https://doi.org/10.1126/science.1203043>
- Whitmire, S. L., & Tobin, P. C. (2006). Persistence of invading gypsy moth populations in the United States. *Oecologia*, *147*, 230–237. <https://doi.org/10.1007/s00442-005-0271-5>
- Wu, Y., Molongoski, J. J., Winograd, D. F., Bogdanowicz, S. M., Louyakis, A. S., Lance, D. R., ... Harrison, R. G. (2015). Genetic structure, admixture and invasion success in a Holarctic defoliator, the gypsy moth (*Lymantria dispar*, Lepidoptera: Erebididae). *Molecular Ecology*, *24*, 1275–1291. <https://doi.org/10.1111/mec.13103>
- Zhou, X., & Stephens, M. (2012). Genome-wide efficient mixed-model analysis for association studies. *Nature Genetics*, *44*, 821–824. <https://doi.org/10.1038/ng.2310>
- Zhou, X., Carbonetto, P., & Stephens, M. (2013). Polygenic modeling with Bayesian sparse linear mixed models. *PLoS Genetics*, *9*, e1003264. <https://doi.org/10.1371/journal.pgen.1003264>
- Zimin, A. V., Puiu, D., Luo, M. C., Zhu, T., Koren, S., Yorke, J. A., ... Salzberg, S. (2017). Hybrid assembly of the large and highly repetitive genome of *Aegilops tauschii*, a progenitor of bread wheat, with the MaSuRCA mega-reads algorithm. *Genome Research*, *27*, 787–792. <https://doi.org/10.1101/gr.213405.116>

SUPPORTING INFORMATION

Additional supporting information may be found online in the Supporting Information section at the end of the article.

How to cite this article: Friedline CJ, Faske TM, Lind BM, et al. Evolutionary genomics of gypsy moth populations sampled along a latitudinal gradient. *Mol Ecol*. 2019;28:2206–2223. <https://doi.org/10.1111/mec.15069>